Casimir forces

S. Reynaud[1] and A. Lambrecht[1]

[1] *Laboratoire Kastler Brossel, CNRS, ENS-PSL Research University, Collège de France, UPMC-Sorbonne Universités, Campus Jussieu, F-75252 Paris, France.*

The present notes are organized as the lectures given at the Les Houches Summer School "Quantum Optics and Nanophotonics" in August 2013. The first section contains an introduction and a description of the current state-of-the-art for Casimir force measurements and their comparison with theory. The second and third sections are a pedagogical presentation of the main features of the theory of Casimir forces for 1-dimensional model systems and for mirrors in 3-dimensional space.

arXiv:1410.2746v1 [quant-ph] 10 Oct 2014

Introduction

The emergence of quantum theory has profoundly altered our conception of space by forcing us to consider it as permanently filled by vacuum field fluctuations [1, 2]. These vacuum fluctuations are electromagnetic fields propagating with the speed of light, as any free field, and corresponding to an energy of half a photon per mode. They have a number of observable consequences in microscopic physics, for example the radiative corrections in subatomic physics [3], the spontaneous emission processes, the Casimir-Polder interaction and Lamb shift in atomic physics [4].

Vacuum fluctuations also have observable mechanical effects in macroscopic physics and the archetype of these effects is the Casimir force between two motionless mirrors. This force was predicted in 1948 by H. B. G. Casimir [5] and soon observed in experiments [6]. Experiments have been improved after years of development and they now reach a good precision [7–10] (more references below). However, the comparison with theoretical predictions has raised difficulties which have been discussed in a large number of papers (references in [11–13]).

This comparison is particularly interesting because of its fascinating interfaces with open questions in fundamental physics. The Casimir effect is connected with the puzzles of gravitational physics through the problem of vacuum energy as well as with the principle of relativity of motion [14]. Effects beyond the Proximity Force Approximation also make apparent the rich interplay of vacuum and geometry [15]. Casimir physics also plays an important role in the tests of gravity at sub-millimeter ranges [16–19]. For scales of the order of the micrometer, such gravity tests are performed by comparing Casimir force measurements with theory and the comparison has to take into account the many differences between real experiments and the idealized case considered initially by Casimir [20].

At the end of this short general introduction, it has also to be stressed that the Casimir and closely related Casimir-Polder forces [21–25] have strong connections with various active domains and interfaces of physics, such as atomic and molecular physics, condensed matter and surface physics, chemical and biological physics, micro- and nano-technology [26, 27].

Outline

The present paper is organized as the lectures given at the Les Houches Summer School in August 2013 : the first section contains an introduction and a description of the current state-of-the-art for experiments and their comparison with theory while the second and third sections are a pedagogical presentation of the main features of the theory of Casimir forces.

Section I begins with a short history of quantum field fluctuations in vacuum. We then review various arguments involved in the comparison with theory of the experiments devoted to the measurement of the Casimir force. As experiments are performed with gold-covered plates, the force depends on non universal properties of the real plates used in the experiments. As they are performed at room temperature, the effect of thermal field fluctuations has to be added to that of vacuum fluctuations. The most precise experiments are performed in the plane-sphere geometry and not in the geometry of two parallel planes whereas the latter is theoretically easier to handle. Finally, surfaces are non ideal, and effects such as roughness, electrostatic patches and contamination affect the comparison between theory and experiment.

Section II contains a simple derivation of the Casimir effect in a model of scalar fields on a 1-dimensional line. This model allows one to introduce the *Quantum Optics* approach to the Casimir effect. This approach is based on the existence of field fluctuations which pervade empty space and exert *radiation pressure* on mirrors at rest in vacuum. The force is thus calculated as the result of different pressures acting on inner and outer sides of the two mirrors which form a cavity. This approach is often also called the *Scattering Formalism* because all properties of the Casimir force are determined by the reflection amplitudes of the fields on the two mirrors [28].

Section III then treats the case of two plane and parallel mirrors at rest in electromagnetic vacuum in 3-dimensional space. It describes the models generally used for the metallic mirrors used in the experiments [29, 30] and discusses the results obtained in this manner. For mirrors characterized by Fresnel reflection amplitudes deduced from a linear and local dielectric function, the Scattering Formalism leads to the same results as Lifshitz's method [31–33]. The section ends up with a presentation of the general scattering formalism which al-

lows one to deal with non specular reflection and arbitrary geometries [34–39]

I. VACUUM FLUCTUATIONS AND CASIMIR FORCES

The birth of quantum vacuum

The classical idealization of absolute empty space was affected by the discovery of black body radiation which is present everywhere at non zero temperature and exerts a pressure onto the boundaries of any cavity. It is precisely for explaining the properties of black body radiation that Planck introduced the first quantum law in 1900 [40] (discussions in [41]).

In modern terms, the first Planck law gives the energy per electromagnetic mode characterized by its frequency $\omega = 2\pi\nu$ as the product of the energy of a single photon $\hbar\omega \equiv h\nu$ by a mean number of photons $\overline{n}$ per mode

$$\overline{E}_{1900} = \overline{n}\hbar\omega \quad , \qquad \overline{n} \equiv \frac{1}{e^{\hbar\omega/k_{\rm B}T} - 1} \ . \tag{1}$$

Unsatisfied with his first derivation, Planck [42] wrote in 1911 a new expression for the mean energy per mode

$$\overline{E}_{1911} = \left(\frac{1}{2} + \overline{n}\right)\hbar\omega \ . \tag{2}$$

The difference between the two Planck laws corresponds to the zero-point energy. Whereas the first law describes a cavity entirely emptied out of radiation at the limit of zero temperature ($\overline{n} \to 0$ when $T \to 0$), the zero-point energy added in the second law persists at zero temperature.

The story of the two Planck laws and of the discussions they raised is related for example in [43]. The arguments used by Planck in 1911 are no longer considered as satisfactory nowadays but an argument which is still valid was proposed by Einstein and Stern in 1913 [44]. In order to state this argument, let us consider the limit for $\overline{E}$ at high temperatures ($k_{\rm B}T \gg \hbar\omega$)

$$\begin{aligned} \overline{E}_{1900} &= \frac{\hbar\omega}{e^{\hbar\omega/k_{\rm B}T} - 1} = k_{\rm B}T - \frac{\hbar\omega}{2} + \frac{(\hbar\omega)^2}{4k_{\rm B}T} + \dots \\ \overline{E}_{1911} &= \frac{\hbar\omega}{2} + \overline{E}_{1900} = k_{\rm B}T + \mathcal{O}\left(\frac{(\hbar\omega)^2}{k_{\rm B}T}\right) \ . \end{aligned} \tag{3}$$

In contrast to the first Planck's law (1) which falls off the correct classical limit by a constant offset $\frac{1}{2}\hbar\omega$, the second Planck's law (2) matches the correct classical limit at high temperatures. This feature is emphasized by the modern writing of this law which has clearly no term linear in $\hbar\omega$ because the right-hand side is an even function of ω (note that $\coth(x) \equiv 1/\tanh(x)$)

$$\overline{E}_{1911} = \left(\frac{1}{2} + \overline{n}\right)\hbar\omega = \frac{\hbar\omega}{2}\coth\frac{\hbar\omega}{2k_{\rm B}T} \ . \tag{4}$$

Debye was the first to insist on observable consequences of zero-point fluctuations in atomic motion, by discussing their effect on the intensities of diffraction peaks [45] whereas Mulliken gave the first experimental proof of these consequences by studying vibrational spectra of molecules [46]. At this point, we may emphasize that these discussions took place before the existence of these fluctuations was confirmed by fully consistent quantum theoretical calculations. Nowadays, vacuum fluctuations are just an immediate consequence of Heisenberg inequalities (see for example references in [47, 48] and in several chapters of the proceedings of this summer school [49]).

The puzzle of vacuum energy

Nernst is credited for having been the first to emphasize in 1916 that zero-point fluctuations should also exist for free electromagnetic fields [50] (discussions in [51]), thus discovering what physicists now call *quantum vacuum*. He also noticed that the associated energy constituted a challenge for gravitation theory. When summing up the zero-point energies over all field modes, a finite energy density is obtained for the first Planck law - this is the solution of the *ultraviolet catastrophe* - but an infinite value is produced from the second law. When introducing a high frequency cutoff, the calculated energy density remains finite but it is still much larger than the mean energy observed in the world around us through gravitational phenomena [52]. Pedagogical derivations and numbers illustrating this major problem are given in [53].

This puzzle has led famous physicists to deny the reality of vacuum fluctuations. In particular, Pauli stated in his textbook on Wave Mechanics [54] (translation from [55]): *At this point it should be noted that it is more consistent here, in contrast to the material oscillator, not to introduce a zero-point energy of $\frac{1}{2}\hbar\omega$ per degree of freedom. For, on the one hand, the latter would give rise to an infinitely large energy per unit volume due to the infinite number of degrees of freedom, on the other hand, it would be principally unobservable since nor can it be emitted, absorbed or scattered and hence, cannot be contained within walls and, as is evident from experience, neither does it produce any gravitational field.*

A part of these statements is simply unescapable: it is just a matter of evidence that the mean value of vacuum energy as predicted by quantum theory does not contribute to gravitation as an ordinary energy. However, we know nowadays that vacuum fluctuations are *scattered* by matter, as shown by the numerous effects of the associated scattering in subatomic [3] and atomic [4] physics. And the Casimir effect discussed in the sequel of this paper may be seen as the manifestation of vacuum fluctuations when being *contained within walls*. Let us note at this point that different points of view coexist about the significance of vacuum fluctuations [55–63].

The puzzle of vacuum energy has been discovered nearly one century ago and it is not yet solved. It has led and still leads to many ideas: for example, a *dark energy length scale* λ=85μm can be defined by setting the cutoff used to calculate the vacuum energy so that it fits the now measured cosmic vacuum energy density [64–66]. It is thus natural to check if gravity could be affected below this dark energy length scale [67–69]. It has been shown in torsion-balance experiments [70] that Yukawa modifications of the gravitational inverse-square law can have a magnitude equal to that of gravity only if their range has a value smaller than 56μm, which discards this kind of ideas under their simplest forms. More possibilities, corresponding for example to power-law modifications associated with compact extra-dimensions [71], are discussed in [17–19].

The search for scale-dependent modifications of the gravity force law are currently pushed down to even smaller ranges and they approach the micrometer distance range where Casimir forces are predominant. For these *Casimir tests* of the gravity law to make sense, the accuracy and reliability of theoretical and experimental values have to be assessed cautiously and independently of each other. In particular, systematic effects have to be identified and eliminated, whenever this is possible. This implies in particular to deal carefully with the many differences between the idealized situation studied by Casimir and the configuration of real experiments [72].

The Casimir force between ideal and real mirrors

In his initial calculation [5], Casimir considered an idealized configuration, with perfectly smooth, flat and parallel plates (see Figure 1) in the limit of zero temperature and perfect reflection. L denotes the distance between the two plates and A their area, supposed to be large enough ($A \gg L^2$).

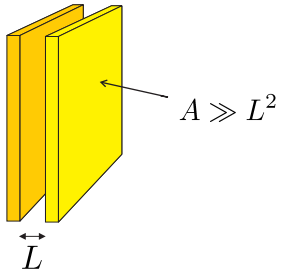

FIG. 1. Configuration considered by Casimir : two perfectly parallel planes placed in vacuum experience an attractive pressure given by (6) under the assumptions of perfect reflection and zero temperature.

He thus obtained expressions for the energy $E_{\rm Cas}$ and force $F_{\rm Cas} \equiv -{\rm d}E_{\rm Cas}/{\rm d}L$ which exhibit a universal behavior associated with the confinement of vacuum energy

$$E_{\rm Cas} = -\frac{\hbar c \pi^2 A}{720 L^3} \quad , \quad F_{\rm Cas} = -\frac{\hbar c \pi^2 A}{240 L^4} \ , \tag{5}$$

where c is the speed of light and $\hbar = h/2\pi$ the reduced Planck constant. The signs have been chosen according to the standard thermodynamical conventions (the relation with thermodynamics of the Casimir effect will be discussed later on). The negative energy corresponds to a binding energy and the negative force to an attractive force, that is also a negative pressure

$$P_{\rm Cas} \equiv \frac{F_{\rm Cas}}{A} = -\frac{\hbar c \pi^2}{240 L^4} \ . \tag{6}$$

The order of magnitude of the pressure is $|P_{\rm Cas}| \sim$1mPa for two mirrors at the distance $L = 1\mu$m typical for Casimir force measurements (see below). The formula (6) describes an extremely rapid increase of the pressure when the distance is decreased, and it would lead to a value $\sim$1TPa typical of strong molecular cohesion when it is extrapolated down to atomic distances $\sim$0.1nm. This means that the Casimir force is a quantum force like molecular cohesion forces, which has a weaker magnitude only because it is measured at distances much larger than typical atomic distances. Note however that formula (6) cannot be used at atomic distances where the ideal assumptions used to derive it are no longer valid, as we explain now.

The effect of imperfect reflection

Indeed, perfectly reflecting mirrors do not exist, except as idealizations giving fair descriptions of reality in limiting cases only. The mirrors used in the experiments are made of metal and they have a good reflection only at frequencies below the plasma frequency. Accounting for their imperfect reflection and its frequency dependence is thus essential for obtaining a reliable theoretical expectation of the Casimir pressure [20]. In other words, the real Casimir pressure depends on the non universal optical properties of the material plates used in the experiments. It can be written as the product of the ideal result (6) by a dimensionless factor which accounts for these optical properties

$$P = P_{\rm Cas} \eta_{\rm P} \ . \tag{7}$$

The expression of $\eta_{\rm P}$ in terms of the optical properties of the mirrors will be given in section III

Most descriptions of the metallic mirrors used in the experiments are based on Fresnel reflection laws at the two interfaces between vacuum and metallic bulks with optical properties described by a linear and local dielectric response function. This dielectric function ε is a sum of contributions corresponding respectively to bound ($\bar{\varepsilon}$) and conduction electrons, the latter being directly related to the conductivity (σ)

$$\varepsilon[\omega] = \bar{\varepsilon}[\omega] + \frac{\sigma[\omega]}{-\imath\omega} \ . \tag{8}$$

Note that functions ε, $\bar{\varepsilon}$ and σ are all defined as reduced quantities, with their SI counterparts being $\varepsilon_0\varepsilon$, $\varepsilon_0\bar{\varepsilon}$ and $\varepsilon_0\sigma$ ($\varepsilon_0 = 1/\mu_0 c^2$ is the vacuum permittivity). With these conventions, ε and $\bar{\varepsilon}$ are dimensionless while σ has the dimension of a frequency.

The dielectric function (8) has to be obtained from optical data [29, 73] as they are tabulated for example for gold in [74]. At low frequencies, $\bar{\varepsilon}$ tends to a constant while the contribution of conduction electrons diverges while σ tends to a constant σ_0. Optical data have then to be extrapolated at low frequencies by using the dissipative Drude model for the conductivity of the metal [75]

$$\sigma_{\rm D}[\omega] = \frac{\omega_{\rm P}^2}{\gamma - \imath\omega} \ . \tag{9}$$

Here $\omega_{\rm P}$ is the plasma frequency and γ the relaxation parameter for conduction electrons. This model meets the well-known fact that gold has a finite static conductivity

$$\sigma_0 = \frac{\omega_{\rm P}^2}{\gamma} \ . \tag{10}$$

For reasons which will become clear in the following, the limiting case of a lossless plasma of conduction electrons ($\gamma = 0$ in (9)) is often considered

$$\sigma_{\rm P}[\omega] = \frac{\omega_{\rm P}^2}{-\imath\omega} \ . \tag{11}$$

This so-called *plasma model* cannot be an accurate description of metallic mirrors. As a matter of fact, it contradicts the fact that gold has a finite static conductivity (10) while also leading to a poorer fit of tabulated optical data than the more general Drude model [29]. However, γ is much smaller than $\omega_{\rm P}$ for a good metal (for example $\gamma \simeq 0.004\omega_{\rm P}$ for gold). As the difference between (9) and (11) is appreciable only at low frequencies $\omega \lesssim \gamma$ where ε is very large for both models, one might expect that it does not affect too much the value of the Casimir force. This naive expectation is met at small distances or low temperatures but not in the general case of arbitrary distances and temperatures, as explained in the following.

The effect of temperature

Most experiments are performed at room temperature, so that the effect of thermal fluctuations has to be added to that of vacuum fields [76–79]. This important point will be discussed in a detailed manner in sections II & III. At this point, we focus on the strong correlation effect obtained between the effects of temperature and dissipation, which has given rise to a large number of contradictory papers (see for example the references in [80–84]).

Boström and Sernelius [85] were the first to remark that, in spite of the naive expectation described in the end of the preceding subsection, dissipation has a large effect on the value of the Casimir force at distances accessible in experiments and at room temperature. Their result is illustrated on Figure 2 where the ratio $\eta_{\rm P}$ giving the real Casimir pressure (7) is drawn for the Drude and plasma models at room temperature (T=300K), using the formulas in [83]. These two models correspond to the dielectric function (8) with $\bar{\varepsilon}$=1 and σ substituted by (9) and (11) respectively. The simplification $\bar{\varepsilon}$=1 does not change the difference between the predictions of the two models and it can also be dropped, by having $\bar{\varepsilon}$ deduced from the optical data. The parameters of the optical models are chosen to match values typical for thick layers of gold ($\omega_{\rm P} = 2\pi c/\lambda_{\rm P}$ with $\lambda_{\rm P}$=136nm and $\gamma/\omega_{\rm P} = 0.004$).

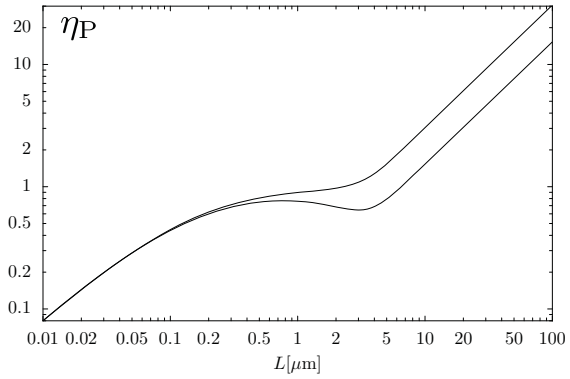

FIG. 2. Variation with distance L of the Casimir pressure shown as the ratio $\eta_{\rm P}$ of the real (P) to the ideal ($P_{\rm Cas}$) Casimir pressure (see eq.(7)). P is smaller than $P_{\rm Cas}$ ($\eta_{\rm P} < 1$) at small distances ($L \lesssim 1\mu$m), due to imperfect reflection, whereas it is larger ($\eta_{\rm P} > 1$) at large distances ($1\mu{\rm m} \lesssim L$), due to the contribution of thermal photons. In the latter large-distance domain, there is a significant difference between the Drude (lower curve) and plasma (upper curve) models, both drawn here for room temperature.

A striking difference appears between the predictions of the two models [85]. These predictions, which are close to each other at short distances, exhibit an increasing difference for distances of the order or larger than 1μm. In particular, the ratio of the plasma to Drude prediction for the Casimir pressure goes to a factor 2 at the limit of large distances. In fact, the result of the plasma model coincides at this limit with that obtained for perfect mirrors whereas the result of the Drude model reaches only half that value. It is worth recalling here that this last result is reproduced by the derivations of Casimir pressures from microscopic models of the metallic mirrors [86–88].

As a matter of principle, there should be no doubt that the Drude model is a better representation of the optical properties of real plates at low frequencies than the plasma model. At this point however, we have to face discrepancies in the comparison between experimental results and theoretical predictions and, unexpectedly, some experimental results appear to lie closer to the predictions of the plasma model than to that of the Drude

model [12]. Before coming to this point, we have still to discuss another important feature of the recent precise experiments which are performed in the plane-sphere geometry and not in the plane-plane geometry in which most calculations are done.

The effect of geometry

The configuration used for most Casimir experiments corresponds to a plane and a sphere, with L the distance of closest approach and R the radius of the sphere, supposed to be large (see Figure 3). The force in this plane-sphere geometry is usually calculated by using the so-called *Proximity Force Approximation* (PFA) [89, 90]. Let us emphasize here that this approximation is valid only at the limit of a very large radius ($R \gg L$) and that the question of its accuracy for a finite value of R/L remains an open question (more discussions on this topic later on).

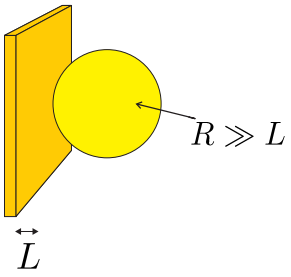

FIG. 3. Configuration for most Casimir experiments : a plane and a spherical mirror placed in vacuum experience an attractive force.

We assume here provisionally that the PFA is precise enough for the purpose of theory-experiment comparison. It follows that the force between the plane and the sphere can be obtained by integrating over the distribution of local inter-plate distances the pressure P calculated in the geometry with two parallel planes. In the plane-sphere geometry, this gives

$$F_{\rm PFA}\left(L\right) = \int_L^\infty {\rm d}A\ P\left(\mathcal{L}\right) \quad , \quad {\rm d}A = 2\pi R\ {\rm d}\mathcal{L}\ , \tag{12}$$

where $P\left(\mathcal{L}\right)$ is the pressure evaluated between two planes at at a distance $\mathcal{L}$ from each other; $\mathcal{L}$ runs over distances larger than the distance of closest approach L and ${\rm d}A$ is the corresponding element of surface.

In the experiment, the gradient G of the Casimir force in the plane-sphere geometry is measured (see the next subsection). This quantity is deduced from (12) as

$$G_{\rm PFA}\left(L\right) \equiv \frac{\partial F_{\rm PFA}}{\partial L} = -2\pi R P\left(L\right)\ . \tag{13}$$

Within PFA, this measurement gives the Casimir pressure evaluated at distance L between two planes, which can then be substituted by the expression (7) (with $\eta_{\rm P}$ to be given in section III).

Casimir experiments

We now present briefly the experimental methods and results. To this aim, we focus our attention on a few experiments : the experiment at IUPUI [8–10] which has been run for ten years, with results pointing to an unexpected conclusion later confirmed at UCR [91], and the experiment in Yale [92] which points to a different conclusion. We also give here a list of other Casimir measurements which have produced information of interest on the topics discussed in this paper [93–112].

The experiment at IUPUI is described in the papers [8–10]. A summary and update can be found in the slides associated with a talk given recently by R.S. Decca at a Pan-American Advanced Study Institute school [113]. The experiment uses dynamic measurements of the resonance frequency of a torsion micro-oscillator. For the free micro-oscillator, that is in the absence of the Casimir force, the resonance frequency is determined by the stiffness coefficient K_0 and the moment of inertia I

$$\omega_0^2 = \frac{K_0}{I}\ . \tag{14}$$

When a gold-covered sphere is approached from the gold-covered plane of the micro-oscillator plate, the effective stiffness is modified as the gradient of the Casimir force G. The resonance frequency is thus shifted to a new value

$$\omega^2 = \frac{K}{I} \quad , \quad K = K_0 - b^2 G\ , \tag{15}$$

where b is the lever arm. As the radius of the sphere is $R \simeq 150\mu$m and the range of distances $0.16\mu{\rm m} < L < 0.75\mu{\rm m}$, the condition $R \gg L$ is met. Using the expression (13) which gives the gradient G within the PFA, and measuring accurately b, I and R, the shift of the squared frequency is then transformed into a reading of the Casimir pressure $P\left(L\right)$ as it would be between two planes at distance L

$$\omega^2 - \omega_0^2 = \frac{b^2}{I} 2\pi R\ P\left(L\right)\ . \tag{16}$$

P is given by (7) and $\eta_{\rm P}$ will be discussed in section III. Note that the separation L between bodies is measured separately through two-color interferometry, up to a global offset adjusted in the data analysis process [9, 10].

When compared with the theoretical prediction, this measurement leads to unexpected conclusions [9, 10]: the measurements appear to agree with the predictions obtained from the lossless plasma model $\gamma = 0$ but to deviate significantly from those deduced from the Drude model which accounts for dissipation (see Fig.1 in [9]). These experiments are performed in a range of distances $0.16\mu{\rm m} < L < 0.75\mu{\rm m}$ where the difference between the predictions of the two models is small. This entails that the problem of accuracy, that is also the control of systematic errors, is a critical issue. However, the deviation of experimental results from theoretical expectations

(based on the Drude model) is clearly larger than the statistical dispersion of these results (bars on Fig.1 in [9]). More details on statistical and systematic errors in this experiment can be found in [9, 10].

Different conclusions are reached in a more recent experiment performed in Yale [92]. This experiment aims at measurements at larger distances $0.7\mu\text{m} < L < 7\mu\text{m}$, where the force is smaller while the thermal contribution and the effect of dissipation are larger (see Fig.2). The experimental technique is based on a torsion balance and uses a much larger sphere $R = 156\text{mm}$, which allows for measurements of weaker pressures. This experiment clearly sees the thermal effect and its results fit the predictions drawn from the dissipative Drude model, after the contribution of the electrostatic patch effect has been subtracted [92]. These new results have to be confirmed by further studies [114]. The main issue in this experiment is that the pressure due to electrostatic patches is larger than that due to Casimir effect, so that a proper modeling of this contribution is critical whereas the patch pattern has not been characterized independently. This is in fact a more general problem since the patch properties have not been measured in other experiments either (more discussions below).

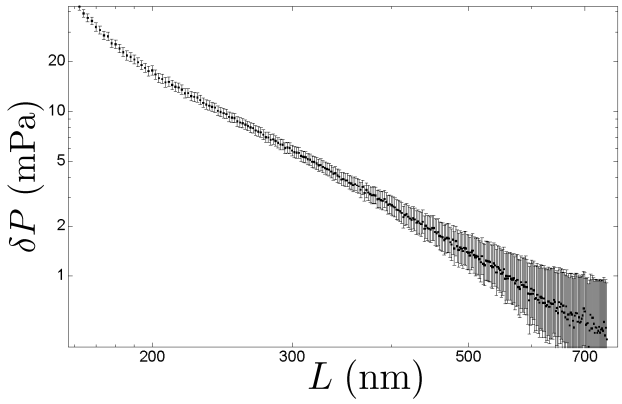

FIG. 4. Difference $\delta P = P_{\text{exp}} - P_{\text{th}}$ between the experimental and theoretical values of the Casimir pressure as a function of the distance L. Experimental values were kindly provided by R.S. Decca and theoretical values calculated by R.O. Behunin *et al* [115], with the Drude model and at room temperature.

Discussion

The conclusion at this point is that the Casimir effect is measured with a good precision in several experiments, with a persisting problem however in terms of accuracy. The results of the most precise experiment, improved over a decade at IUPUI and confirmed recently at UCR, appear to favor theoretical predictions obtained with the lossless plasma model and to deviate from the predictions obtained with the best motivated model, that is the dissipative Drude model. The Yale experiment fits predictions drawn from this Drude model, after the subtraction of a large contribution of the electrostatic patch effect. For the IUPUI experiment, the pressure difference goes up to $\sim$50mPa at the smallest distances $\sim$160nm where the pressure itself is $\sim$1000mPa, which entails that the accuracy is certainly not at the 1% level, as has been occasionally claimed.

The difference $\delta P = P_{\text{exp}} - P_{\text{th}}$ between the experimentally measured (P_{exp}) and theoretically predicted (P_{th}) values of the Casimir pressure is drawn on Fig.4 as a function of the distance L. Experimental values and error bars correspond to data kindly provided by R.S. Decca [9, 10, 113]. Theoretical values were calculated by R.O. Behunin *et al* in [115], using the optical data of gold extrapolated at low frequencies to a Drude model, and at room temperature. Systematic corrections were done in [115] as in [9, 10] and similar results obtained. The discrepancy clearly appears on Fig.4 and it is of particular importance in the context of gravity tests at submillimeter ranges [18, 19]. The deviation seen on Fig.4 does not look like a Yukawa law, but it certainly looks like a combination of power laws !

This discrepancy between theory and experiment may have various origins, in particular artifacts in the experiments or inaccuracies in the theoretical evaluations. They may also come from yet unmastered systematic effects in the comparison between experimental data and theoretical predictions. They could in principle be the first hint of the existence of new forces beyond the standard model, though such a strong statement should only be considered after a cautious examination of the more mundane explanations associated in particular with systematic effects.

The theoretical formula used to calculate the Casimir pressure between real plates will be derived in section III. It will reproduce the ideal Casimir expression at the limits of perfect reflection and null temperature while being valid at any temperature for any model of mirrors obeying well motivated physical properties [28, 29], including the case of dissipative mirrors [30]. When the reflection amplitudes are deduced from the Fresnel laws, and semi-infinite bulk mirrors are characterized by a linear and local dielectric response function, the results reproduce those of I.E. Dzyaloshinskii, E.M. Lifshitz and L.P. Pitaevskii [31–33]. It then remains to specify this dielectric function and its low-frequency behavior. Here, it is worth emphasizing that the Drude model, though being obviously much better motivated than the lossless plasma model, is not a very accurate description of conduction phenomena in real metals. More detailed descriptions can be considered, which can for example be determined from microscopic models of conduction in metals. Attempts in this direction and discussions can be found for example in [116–122]. To date, they have been unable to explain the discrepancy.

A possible source of systematic error is the use of the

Proximity Force Approximation (PFA) in order to derive expressions for the plane-sphere geometry from those known from the plane-plane geometry. This approximation is expected to be valid at the limit where the aspect ratio $x \equiv L/R$ goes to zero. Even in this case, the accuracy of the PFA for a finite value of x remains an open question after the remarkable advances made recently on this topic [123], which will be described in section III. The question remains open, even though most specialists would probably bet that the deviation from PFA is not able to bridge the gap between experiment and theory. Other possible sources of systematic error involve the effects of surface physics on Casimir experiments. The problem of surface roughness has been studied in a thorough manner [124–129].

Electrostatic patches and contamination

Electrostatic patches and contamination, already alluded to, are a worrying source of such systematic effects, discussed in the sequel of this section. Electrostatic patches have been known for a long time to be a source of worries for a large number of high precision measurements [130–143], and in particular for Casimir experiments [144–148] and short-range gravity tests [18]. The patch effect is due to the fact that the surface of a metallic plate cannot be an equipotential as it is made of micro-crystallites with different work functions. For clean metallic surfaces studied by the techniques of surface physics, the resulting *voltage roughness* is correlated to the *topography roughness* as well as to the orientation of micro-crystallites [149]. For surfaces exposed to air, the situation is changed due to the unavoidable contamination by adsorbents, which spread out the electrostatic patches, enlarge correlation lengths and reduce voltage dispersions [150].

The pressure due to electrostatic patches between two planes can be computed by solving the Poisson equation [144]. Its evaluation depends on the spectra describing the correlations of the patch voltages or, equivalently on the associated noise spectra $C(k)$, with k a patch wave-vector. In analysis of the patch pressure devoted to Casimir experiments up to recently, the spectrum was assumed to be flat between two *sharp cutoffs* at a minimum wave-vector $k_{\rm min}$ and a maximum one $k_{\rm max}$. Assuming furthermore that $k_{\rm min}$ and $k_{\rm max}$ were given by the grain size distribution measured with an Atomic Force Microscope (AFM), it was concluded that the patch pressure was much smaller than the discrepancy between experiment and theory [8–10].

A *quasi-local* model has recently been proposed with the aim of proposing a much better motivated representation of patches [115]. The model is based on a tessellation of the sample surface and a random assignment of the voltage on each patch. It produces a smooth spectrum different from the sharp-cutoff model used in previous analysis since there is now contributions to the patch pressure coming from arbitrary low values of k, even if the patch size distribution has an upper bound. When the patch effect is estimated with the parameters deduced from the grain size distribution as in [8, 9], a much larger contribution of patches is obtained. In fact, the calculated patch pressure is now larger than the residuals between experimental data and theoretical predictions, which means that patches could be a crucial systematic effect for Casimir force measurements [115].

As the computed patch pressure is model dependent, it seems natural to try to find a model between the two cases presented above which would reproduce at least qualitatively the residuals. By varying the parameters of the quasi-local model, it was found in [115] that the output of the model depended mainly on two parameters, the size of largest patches $\ell_{\rm patch}^{\rm max}$ and the rms voltage dispersion $V_{\rm rms}$ and that a best-fit on these two parameters produced a qualitative agreement between the residuals and the patch pressure. The best-fit values for the parameters $\ell_{\rm patch}^{\rm max}$ and $V_{\rm rms}$ are quite different from those obtained by identifying patch and grain sizes. With $\ell_{\rm patch}^{\rm max}$ larger than the maximum grain size and $V_{\rm rms}$ smaller than the rms voltage which would be associated with random orientations of clean micro-crystallites, these values are however compatible with a contamination of metallic surfaces, which had to be expected anyway.

It follows that the difference between IUPUI experimental data and theoretical predictions can be fitted at least qualitatively by a simple model for electrostatic patches. This conclusion is however only the result of a fit, with the parameters of the patch model not measured independently. In order to reach a firm conclusion, the patch spectrum has to be measured independently, by using the dedicated technique of Kelvin probe force microscopy (KPFM) which is able to achieve the necessary size and voltage resolutions [151, 152]. When these characteristics are available, the contribution of the patches to the Casimir measurements can be evaluated and unambiguously subtracted when comparing theory and experiments.

Preliminary results of such characterizations have recently been published [153]. Note that the evaluation of force was done for the plane-sphere geometry [154].

II. A SIMPLE DERIVATION OF THE CASIMIR EFFECT IN ONE DIMENSION

The present section II contains a derivation of the Casimir effect in a model of scalar fields propagating along the two directions on a 1-dimensional line. Within this simple model which lays the basis for more complicated calculations to appear in the next section, we introduce the *Quantum Optics* approach to the Casimir effect. The approach is based on the scattering of vacuum field fluctuations obtained in the ground state of the associated *Quantum Field Theory*. Each mirror is described by a scattering operator [155, 156] which is reduced here to

a 2×2 matrix containing reflection and transmission amplitudes. Two mirrors form a Fabry-Perot cavity with all field transformations deduced from the two elementary scattering matrices. The Casimir force then results from the difference of radiation pressures exerted onto the inner and outer sides of the mirrors by the vacuum field fluctuations. Equivalently, the Casimir free energy can be written as the shift of field energy due to the presence of the Fabry-Perot cavity [56, 157]. The formula obtained in this manner is valid and regular at thermal equilibrium at any temperature and for any optical model of mirrors obeying causality and high frequency transparency properties.

The radiation pressure interpretation of the Casimir force was presented for perfect mirrors in [158] and extended to the case of real mirrors [28]. The calculations were then systematically expanded in particular for applications to the problem of the *Dynamical Casimir effect* [159–166]. It has also served as a basis for the Scattering Formalism for the static Casimir effect [30, 34] of which we will give a pedagogical presentation in the following.

A. Quantum field theory on the one-dimensional line

We consider here quantum field theory on the one-dimensional line, that is also quantum field theory in two-dimensional space-time (one time coordinate t, one space coordinate x). The field propagation is thus described by the d'Alembert's wave equation, originally written for the propagation of transverse vibrations of a string, and which also describes many wave phenomena such as electrical propagation in a transmission line, acoustic wave and so on.

Propagation equation on the one-dimensional line

We write it here for a single vibration described by the scalar potential $\Phi(x,t)$

$$\frac{\partial^2\Phi}{\partial t^2}-c^2\frac{\partial^2\Phi}{\partial x^2}=0\ . \tag{17}$$

The general solution to this equation is given by the d'Alembert's formula, that is the superposition of rightward (φ^+) and leftward (φ^-) traveling waves propagating at the velocity c in opposite directions along the x-axis

$$\Phi(t,x)=\varphi^+\left(u_+\right)+\varphi^-\left(u_-\right)\ , \tag{18}$$

where $u_\pm$ are called today the light cone variables

$$u_+\equiv t-\frac{x}{c}\quad ,\quad u_-\equiv t+\frac{x}{c}\ . \tag{19}$$

In this simplest version of field theory, there is one normal mode for each frequency $\omega\in[0,\infty]$ and each propagation direction $\eta=\pm 1$. The standard methods of quantum field theory [3, 4] then allow one to write the rightward (φ^+) and leftward (φ^-) traveling waves as Fourier decompositions over canonical mode operators

$$\varphi^\eta\left(u\right)=\int_0^\infty\frac{\mathrm{d}\omega}{2\pi}\sqrt{\frac{\hbar}{2\omega}}\left(a_{\omega,\eta}e^{-\imath\omega u}+a^\dagger_{\omega,\eta}e^{\imath\omega u}\right)\ . \tag{20}$$

Annihilation and creation operators $a_{\omega,\eta}$ and $a^\dagger_{\omega,\eta}$ correspond respectively to positive and negative frequencies in the decompositions (20). Note that the fields in space-time $\varphi^\eta(u)$ are real-valued, so that annihilation and creation operators are hermitian conjugate of each other. They obey the following canonical commutation relations

$$\begin{aligned}\left[\,a_{\omega,\eta}\,,\,a^\dagger_{\omega',\eta'}\,\right]&=2\pi\delta\left(\omega-\omega'\right)\delta_{\eta,\eta'}\ ,\\ \left[\,a_{\omega,\eta}\,,\,a_{\omega',\eta'}\,\right]&=\left[\,a^\dagger_{\omega,\eta}\,,\,a^\dagger_{\omega',\eta'}\,\right]=0\ .\end{aligned} \tag{21}$$

The Hamiltonian $\mathcal{H}$ for the d'Alembert's wave equation (17) is the integral over space of the energy density $e(t,x)$

$$\mathcal{H}=\int\mathrm{d}x\ e(t,x)\ ,\ e\equiv\frac{1}{2}\left(\frac{\partial\Phi}{\partial t}\right)^2+\frac{c^2}{2}\left(\frac{\partial\Phi}{\partial x}\right)^2. \tag{22}$$

Using the d'Alembert's formula (18) for fields, one derives another d'Alembert's formula describing the general energy density as the superposition of rightward and leftward traveling flows

$$e(t,x)=e^+\left(u_+\right)+e^-\left(u_-\right)\ ,\ e^\eta\left(u_\eta\right)=\left(\frac{\partial\varphi^\eta}{\partial u_\eta}\right)^2 \tag{23}$$

Vacuum and thermal fluctuations

Vacuum $|\,\mathrm{vac}\,\rangle$ is the fundamental state of quantum field with an infinite number of modes each containing no photons. This means that all annihilation operators vanish in this state while creation operators have their action determined by the commutation relations (21).

In the following, we use the correlation functions of vacuum fields which are deduced from these elementary properties

$$\begin{aligned}\langle\,a_{\omega,\eta}\,\rangle_{\mathrm{vac}}&=\left\langle\,a^\dagger_{\omega,\eta}\,\right\rangle_{\mathrm{vac}}=0\ ,\\ \left\langle\,a_{\omega,\eta}a^\dagger_{\omega',\eta'}\,\right\rangle_{\mathrm{vac}}&=2\pi\delta\left(\omega-\omega'\right)\delta_{\eta,\eta'}\ ,\\ \left\langle\,a^\dagger_{\omega,\eta}a_{\omega',\eta'}\,\right\rangle_{\mathrm{vac}}&=0\ ,\\ \langle\,a_{\omega,\eta}a_{\omega',\eta'}\,\rangle_{\mathrm{vac}}&=\left\langle\,a^\dagger_{\omega,\eta}a^\dagger_{\omega',\eta'}\,\right\rangle_{\mathrm{vac}}=0\ ,\end{aligned} \tag{24}$$

where $\langle\ldots\rangle_{\mathrm{vac}}\equiv\langle\,\mathrm{vac}\,|\,\ldots\,|\,\mathrm{vac}\,\rangle$. Higher-order correlation functions are deduced from the fact that vacuum fields may be dealt with as Gaussian random variables.

In a state at thermal equilibrium at temperature T, the first and last lines in (24) are unchanged whereas the second line is changed to

$$\begin{aligned}\left\langle\,a_{\omega,\eta}a^\dagger_{\omega',\eta'}\,\right\rangle_{\mathrm{therm}}&=2\pi\delta\left(\omega-\omega'\right)\delta_{\eta,\eta'}\left(1+\overline{n}\right)\ ,\\ \left\langle\,a^\dagger_{\omega,\eta}a_{\omega',\eta'}\,\right\rangle_{\mathrm{therm}}&=2\pi\delta\left(\omega-\omega'\right)\delta_{\eta,\eta'}\ \overline{n}\ ,\end{aligned} \tag{25}$$

where $\langle \dots \rangle_{\rm therm} \equiv \langle \, {\rm therm} \, | \dots | \, {\rm therm} \, \rangle$ while $\overline{n}$ is the mean photon number in Planck's law (2). Note that (25) is reduced to (24) when $T \to 0$. Note also that all field commutators are unchanged, which is consistent with the fact that they are directly connected to the propagators.

Using the Fourier decompositions (20) of the fields and the correlation functions (25), we deduce that the mean values of energies densities (23) have the following spectral decompositions in the general case ($T \neq 0$)

$$\begin{aligned} \langle \, e^{\eta} \, (u) \, \rangle_{\rm therm} &= \int_0^\infty \frac{{\rm d}\omega}{2\pi} \int_0^\infty \frac{{\rm d}\omega'}{2\pi} \sqrt{\frac{\hbar\omega}{2}} \sqrt{\frac{\hbar\omega'}{2}} \\ &\times \left\langle \, a_{\omega,\eta} a^\dagger_{\omega',\eta'} + a^\dagger_{\omega,\eta} a_{\omega',\eta'} \, \right\rangle_{\rm therm} \\ &= \int_0^\infty \frac{{\rm d}\omega}{2\pi} \frac{\hbar\omega}{2} \, (1 + 2\overline{n}) \ . \end{aligned} \tag{26}$$

This is the modern expression of the second Planck's law [42] for the energy per mode given as the sum of vacuum and thermal contributions (compare with (2)). The limit of zero temperature corresponds to $\overline{n} = 0$ in this expression.

B. One mirror on a 1d line

We now consider the situation where one mirror is placed into vacuum at a position q_1 (see Fig.5).

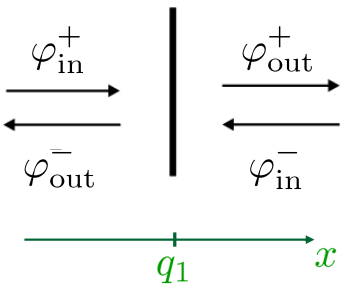

FIG. 5. Schematic representation of a mirror at position q_1 on a 1d line : this mirror is a point-like scatterer which couples rightward and leftward propagating waves.

Scattering by one mirror on a 1d line

The general solution is in this case a generalized d'Alembert's formula with different expressions for fields on the lefthand ($\Phi_{\rm L}$) and righthand ($\Phi_{\rm R}$) sides of the mirror

$$\begin{aligned} \Phi(t,x) &= \Phi_{\rm L}(t,x) + \Phi_{\rm R}(t,x) \ , \\ \Phi_{\rm L}(t,x) &= \varphi^+_{\rm in}(u_+) + \varphi^-_{\rm out}(u_-) \quad , \quad x < q_1 \ , \\ \Phi_{\rm R}(t,x) &= \varphi^+_{\rm out}(u_+) + \varphi^-_{\rm in}(u_-) \quad , \quad q_1 < x \ . \end{aligned} \tag{27}$$

The symbol + and − represent as previously rightward and leftward propagation while the symbols in and out correspond to incoming and outgoing traveling waves. These waves are coupled by scattering on the mirror.

For the limiting case of perfectly reflecting mirrors, the field Φ vanishes at the left and right sides of the mirrors. Output fields are then easily deduced from input ones as $\varphi^\pm_{\rm out}(t,q_1) = -\varphi^\mp_{\rm in}(t,q_1)$. In Fourier space, this is written as a scattering process with reflection amplitudes having a unit modulus and a phase determined by the position of the mirror, $\varphi^\pm_{\rm out}[\omega] = -e^{\mp 2ikq_1} \varphi^\mp_{\rm in}[\omega]$ with $k \equiv \omega/c$. As the scattering process preserves the frequency for a motionless mirror, these equations could as well have been written for annihilation ($\omega > 0$) and creation ($\omega < 0$) operators.

Real mirrors on a 1d line

Real mirrors cannot be perfectly reflecting at all frequencies. They are described by a more general scattering matrix containing transmission as well as reflection amplitudes (with $k \equiv \omega/c$)

$$\begin{aligned} \begin{pmatrix} \varphi^+_{\rm out}[\omega] \\ \varphi^-_{\rm out}[\omega] \end{pmatrix} &= S_1[\omega] \begin{pmatrix} \varphi^+_{\rm in}[\omega] \\ \varphi^-_{\rm in}[\omega] \end{pmatrix} \ , \\ S_1[\omega] &= \begin{pmatrix} t_1[\omega] & r_1[\omega] e^{-2ikq_1} \\ r_1[\omega] e^{2ikq_1} & t_1[\omega] \end{pmatrix} \ . \end{aligned} \tag{28}$$

The scattering amplitudes r_1 and t_1 have been defined for a mirror located at $x = 0$ and the general case then obtained by introducing the phases $e^{\mp 2ikq_1}$ determined by the position of the mirror. We have considered the particular case of a symmetrical scattering matrix for a mirror located at $x = 0$. A more general treatment would not change any important result in the following.

The scattering matrix preserves frequency since energy is conserved for a stationary scattering but it depends on frequency as a consequence of fundamental physical properties [28]. The scattering process considered here obeys the following properties (the unitarity assumption, valid only for lossless mirrors, will be released later on)

1. Fields are real in the time domain, so that $S[\omega]^\dagger = S[-\omega]$, that is also $t_1[\omega]^* = t_1[-\omega]$ and $r_1[\omega]^* = r_1[-\omega]$;

2. The scattering process obeys causality, so that the amplitudes can be prolongated as analytical functions in the upper half of the complex plane (more details below);

3. The scattering process obeys unitarity, so that $S[\omega] S[\omega]^\dagger = \mathcal{I}$, that is also $|r_1[\omega]|^2 + |t_1[\omega]|^2 = 1$ and $t_1[\omega] r_1[\omega]^* + r_1[\omega] t_1[\omega]^* = 0$;

4. Reflection tends to vanish at the high-frequency limit $\lim_{\omega\to\infty} S_1[\omega] \to \mathcal{I}$, so that $\lim_{\omega\to\infty} t_1[\omega] \to 1$ and $\lim_{\omega\to\infty} r_1[\omega] \to 0$.

These general properties may be illustrated with an example, which corresponds in particular to a transmission

line with a localized impedance mismatch [164]. For this simple example, the d'Alembert's wave equation (17) is changed to

$$\frac{\partial^2\Phi}{\partial t^2} - c^2\frac{\partial^2\Phi}{\partial x^2} + 2c\Omega\delta(x-q_1)\Phi(t,q) = 0 \ , \qquad (29)$$

and the solution obtained as (28) with

$$r_1[\omega] = \frac{\Omega}{i\omega-\Omega} \quad , \quad t_1[\omega] = \frac{i\omega}{i\omega-\Omega} \ . \qquad (30)$$

The general properties (1-4) enumerated in the preceding paragraph can easily be checked out. The parameter Ω appears as the physical cutoff above which reflection tends to vanish. The limit of perfect reflection can be defined by the case of large values of Ω. It has been shown that this definition allows one to escape the difficulties encountered when studying perfectly reflecting mirrors [161, 162].

Force on one mirror on the 1d line

We come now to the evaluation of the force acting on the mirror represented on figure 5. To this aim, we first study the energy flows in the same situation, as sketched on figure 6.

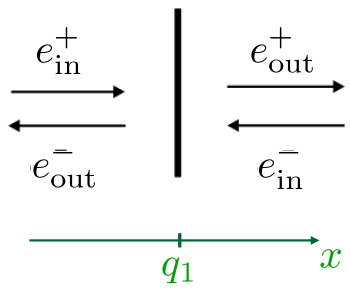

FIG. 6. Schematic representation of energy flows on a 1d line due to scattering on a mirror at position q_1 (see Fig.5).

The general solution is now a d'Alembert's formula (23) for energy densities with different expressions on the lefthand ($e_{\rm L}$) and righthand ($e_{\rm R}$) sides of the mirror

$$\begin{aligned} e(t,x) &= e_{\rm L}(t,x) + e_{\rm R}(t,x) \ , \qquad (31)\\ e_{\rm L}(t,x) &= e^+_{\rm in}(u_+) + e^-_{\rm out}(u_-) \quad , \quad x < q_1 \ ,\\ e_{\rm R}(t,x) &= e^+_{\rm out}(u_+) + e^-_{\rm in}(u_-) \quad , \quad q_1 < x \ . \end{aligned}$$

Similar expressions can be written for the momentum densities by just putting a sign η in front of energy densities e^η. The force on the mirror is then deduced from a momentum balance upon scattering and it is found to be proportional to the difference of the energy densities $e_{\rm L}(t,q)$ and $e_{\rm R}(t,q)$ on the lefthand and righthand sides of the mirror [159].

In the limiting case of perfectly reflecting mirrors, the field Φ vanishes at the left and right sides of the mirrors. Output fields are then easily deduced from input ones as $e^\pm_{\rm out}(t,q_1) = e^\mp_{\rm in}(t,q_1)$, and the force thus obtained as $F(t) = 2\left(e^+_{\rm in}(t,q) - e^-_{\rm in}(t,q)\right)/c$. The mean values $\left\langle e^\pm_{\rm in}(t,q)\right\rangle_{\rm therm}$ of leftward and rightward energy densities are infinite (see (26)). But these mean values are also equal for leftward and rightward densities, so that the force on the mirror is zero $\langle F\rangle_{\rm therm} = 0$.

This result crucially depends on the fact that we have evaluated the mean force on a mirror at rest. There exist non vanishing fluctuations of force on the mirror, as well as a non null mean force for a moving mirror [159].

Force on one real mirror

In the general case of a non perfect mirror, the same result is proven by the following reasoning. First, the force is deduced from the momentum balance upon scattering and the expressions (31) of energy densities

$$\begin{aligned} F(t) &= \frac{e_{\rm L}(t,q) - e_{\rm R}(t,q)}{c} \qquad (32)\\ &= \frac{e^+_{\rm in}(t,q) + e^-_{\rm out}(t,q) - e^+_{\rm out}(t,q) - e^-_{\rm in}(t,q)}{c} \ . \end{aligned}$$

Then, the mean energy densities are calculated by using the expressions (23) of energy densities and the description (28) of the scattering process. From the unitarity of the $S-$matrix, one deduces that mean radiation pressures are still equal on the two sides (equation written at thermal equilibrium at temperature T)

$$\begin{aligned} \left\langle\, e^+_{\rm out}\,\right\rangle &= \left\langle\, e^-_{\rm out}\,\right\rangle = \left\langle\, e^+_{\rm in}\,\right\rangle = \left\langle\, e^-_{\rm in}\,\right\rangle \\ &= \int_0^\infty \frac{{\rm d}\omega}{2\pi}\,\hbar\omega\left(\frac{1}{2}+\overline{n}\right) \ , \qquad (33) \end{aligned}$$

so that the mean value of the force still vanishes

$$\left\langle\, F\,\right\rangle = 0 \ . \qquad (34)$$

C. Two mirrors on the 1d line

The situation changes fundamentally as soon as we consider that there are two mirrors present on the 1d line, which form a Fabry-Perot cavity. There is now a difference between the inner and outer sides of the mirrors, as sketched on Figure 7.

Scattering by a cavity on a 1d line

The spatial positions of the two mirrors are denoted q_1 and q_2 with the length of the cavity $L \equiv q_2 - q_1 > 0$. Each mirror couples rightward and leftward traveling waves. In contrast with the case of one mirror, the fields undergo multiple scattering and there appears an intra-cavity region. The general solution for the fields is now written with different expressions for fields on the lefthand ($\Phi_{\rm L}$)

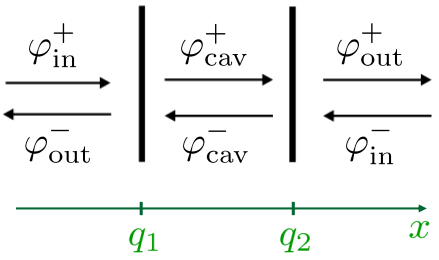

FIG. 7. Schematic representation of the scattering of fields by two mirrors at positions q_1 and q_2 on a 1d line.

and righthand ($\Phi_{\rm R}$) sides of the cavity and those ($\Phi_{\rm C}$) within the cavity

$$\begin{aligned}\Phi(t,x) &= \Phi_{\rm L}(t,x) + \Phi_{\rm C}(t,x) + \Phi_{\rm R}(t,x)\ , \\ \Phi_{\rm L}(t,x) &= \varphi^+_{\rm in}(u_+) + \varphi^-_{\rm out}(u_-)\ ,\ x < q_1\ , \\ \Phi_{\rm C}(t,x) &= \varphi^+_{\rm cav}(u_+) + \varphi^-_{\rm cav}(u_-)\ ,\ q_1 < x < q_2\ , \\ \Phi_{\rm R}(t,x) &= \varphi^+_{\rm out}(u_+) + \varphi^-_{\rm in}(u_-)\ ,\ q_2 < x\ .\end{aligned} \tag{35}$$

The scattering effect of the cavity has now to be described by two matrices, instead of one in the one mirror case, a global scattering matrix S which gives the output fields in terms of the input ones, and a resonance matrix R which gives the intra-cavity fields

$$\begin{aligned}\begin{pmatrix}\varphi^+_{\rm out}\\ \varphi^-_{\rm out}\end{pmatrix} &= S\begin{pmatrix}\varphi^+_{\rm in}\\ \varphi^-_{\rm in}\end{pmatrix}\ , \\ \begin{pmatrix}\varphi^+_{\rm cav}\\ \varphi^-_{\rm cav}\end{pmatrix} &= R\begin{pmatrix}\varphi^+_{\rm in}\\ \varphi^-_{\rm in}\end{pmatrix}\ .\end{aligned} \tag{36}$$

Scattering and resonance matrices

The global $S-$matrix can be evaluated from the elementary matrices S_1 and S_2 associated with the two mirrors and the free propagation phase-shifts. The results can be written as follows (all amplitudes depend on $\omega \equiv ck$)

$$S = \frac{1}{d}\begin{pmatrix} t_1t_2 & dr_2e^{-ikL} + t_2^2r_1e^{ikL} \\ dr_1e^{-ikL} + t_1^2r_2e^{ikL} & t_1t_2\end{pmatrix}\ . \tag{37}$$

The denominator d is an important function, with its zeros corresponding to the resonances of the cavity,

$$d[\omega] = 1 - r[\omega]e^{2ikL}\quad ,\quad r[\omega] \equiv r_1[\omega]r_2[\omega]\ . \tag{38}$$

For the problem under consideration, the global $S-$matrix obeys the same properties as the elementary matrices S_1 and S_2. In particular, it is unitary

$$S[\omega]S[\omega]^\dagger = \mathcal{I}\ . \tag{39}$$

The resonance matrix can be deduced from the elementary matrices S_1 and S_2 associated with the two mirrors and the free propagation phase-shifts. The results are obtained as (amplitudes depend on ω and expressions are simplified by assuming $q_2 = -q_1 = L/2$)

$$R = \frac{1}{d}\begin{pmatrix} t_1 & t_2^2r_1e^{ikL} \\ t_1^2r_2e^{ikL} & t_2\end{pmatrix}\ . \tag{40}$$

The resonance matrix shares some of the properties listed above with the $S-$matrix but it is not unitary. It turns out that $RR^\dagger$ can be written [160]

$$\begin{aligned}R[\omega]R[\omega]^\dagger &= \mathcal{I} + Q[\omega] + Q[\omega]^\dagger\ , \\ Q &= \frac{1}{d}\begin{pmatrix} r_1r_2e^{2ikL} & r_1e^{ikL} \\ r_2e^{ikL} & r_1r_2e^{2ikL}\end{pmatrix}\ .\end{aligned} \tag{41}$$

D. Casimir force on the 1d line

We now evaluate the energy densities and the forces in the case of two mirrors on the 1d line.

Energy densities

The general solution for the energy densities is now written as in (31), considering the configuration sketched on Figure 7 for the cavity.

$$\begin{aligned}e(t,x) &= e_{\rm L}(t,x) + e_{\rm C}(t,x) + e_{\rm R}(t,x)\ , \\ e_{\rm L}(t,x) &= e^+_{\rm in}(u_+) + e^-_{\rm out}(u_-)\ ,\ x < q_1\ , \\ e_{\rm C}(t,x) &= e^+_{\rm cav}(u_+) + e^-_{\rm cav}(u_-)\ ,\ q_1 < x < q_2\ , \\ e_{\rm R}(t,x) &= e^+_{\rm out}(u_+) + e^-_{\rm in}(u_-)\ ,\ q_2 < x\ .\end{aligned} \tag{42}$$

We deduce expressions for the forces acting on each mirror 1 or 2, obtained as differences of the radiation pressures on the lefthand and righthand sides of the mirror (compare with (32))

$$\begin{aligned}F_1(t) &= e_{\rm L}(t,q_1) - e_{\rm C}(t,q_1)\ , \\ F_2(t) &= e_{\rm C}(t,q_2) - e_{\rm R}(t,q_2)\ .\end{aligned} \tag{43}$$

The energy densities on the outer sides of the cavity have the same expressions as in the one-mirror case, provided that the scattering matrix (37) of the cavity is used. As this global $S-$matrix is unitary (see (39)), one deduces that the mean energy densities on the outer sides are still given by equations (33). Hence, they are infinite but equal on the two sides of the cavity so that the mean value of the global force on the cavity vanishes

$$\langle\, F_1 + F_2\,\rangle = 0\ . \tag{44}$$

Intra-cavity energy densities

The situation is different for the energy densities on the intra-cavity sides of the mirrors, since their calculation is now determined by the properties of the resonance

matrix. Using the property (41), one deduces that the mean values of these energy densities is given by [160]

$$\langle\, e^+_{\rm cav}\,\rangle = \langle\, e^-_{\rm cav}\,\rangle = \int_0^\infty \frac{{\rm d}\omega}{2\pi}\,\hbar\omega\left(\frac{1}{2}+\overline{n}\right)\;g[\omega]\;, \quad (45)$$

where $g[\omega]$ is the common value of the diagonal elements in the matrix $RR^\dagger$

$$g[\omega] \equiv 1 + f[\omega] + f[\omega]^* = \frac{1-|r|^2}{|1-r\,e^{2ikL}|^2}\;,$$
$$f[\omega] \equiv \frac{re^{2ikL}}{1-re^{2ikL}}\;. \quad (46)$$

The real function $g[\omega]$ represents the modification of the energy density inside the cavity with respect to that outside the cavity, which is in fact identical for input and output fields. The same result would have been obtained for a classical calculation with an input field at frequency ω. Here this function $g[\omega]$ describes the change of energy densities for vacuum as well as thermal fluctuations. Its relation (46) to the *closed loop function* $f[\omega]$ will be used in the following to transform the expression of the Casimir force.

Casimir force as a result of radiation pressures

Collecting these results, one deduces the following expression of the Casimir force, defined as the mean force on the righthand mirror or the opposite of that on the lefthand mirror (see (44)),

$$F \equiv \langle\, F_2\,\rangle = -\,\langle\, F_1\,\rangle = \int_0^\infty \frac{{\rm d}\omega}{2\pi c}\,\hbar\omega\,(1+2\overline{n})\,(g[\omega]-1)\;. \quad (47)$$

This expression is obtained as the difference of radiation pressures (45) and (33) on the inner and outer sides of the mirrors.

Resonant frequencies correspond to an increase of energy in the cavity ($g > 1$) and they produce repulsive contributions to the Casimir force. In contrast, frequencies out of resonance correspond to a decrease of energy in the cavity ($g < 1$) and they produce attractive contributions to the Casimir force. The net force is the integral of these contributions over all modes. This interpretation of the Casimir force as a result of radiation pressures of vacuum and thermal fluctuations produces a final expression which is finite for any properly defined model of mirrors [28]. This is seen more easily by using causality properties to rewrite (47) as an integral over imaginary frequencies. Let us stress at this point that this rewriting is just a mathematical transformation which does not affect the physical content of (47). The rewriting will however spoil its direct intelligibility as imaginary frequencies do not correspond to physical modes.

Casimir force as an integral over imaginary frequencies

One now rewrites the Casimir force as an integral over imaginary frequencies by using the causality properties of the scattering amplitudes. We give here a simplified description (a more general derivation can be found in [167]).

We first write the Casimir force (47) as the real part of a complex integral F_r defined over the positive part $\mathbb{R}^+$ of the real axis

$$F = F_r + F_r^*\;,$$
$$F_r \equiv \int_0^\infty \frac{{\rm d}z}{2\pi c}\;\hbar z\;f[z]\;\coth\frac{\hbar z}{2k_{\rm B}T}\;. \quad (48)$$

We have used the relation (46) between g and f, substituted the frequency ω by a complex variable z running over $\mathbb{R}^+$. We have also replaced $1+2\overline{n}[\omega]$ by its explicit form (4). Now the closed loop function $f[z]$ is defined from causal reflection amplitudes and propagation phases. Considered as a function of $z \in \mathbb{C}$, it has poles in the lower half part of the complex plane which correspond to resonances of the Fabry-Perot cavity, while it is analytical in the upper half part of the complex plane ${\rm Im}\,z \geq 0$. Meanwhile the function $\coth(\hbar z/2k_{\rm B}T)$ is analytical in the right half part of the complex plane ${\rm Re}\,z > 0$ but has poles at the Matsubara frequencies which are regularly spaced on the imaginary axis [168]

$$z_n = \imath\xi_n \quad , \quad \xi_n = n\xi_1 \quad , \quad \xi_1 = \frac{2\pi k_{\rm B}T}{\hbar}\;. \quad (49)$$

It follows that the integral F_r can be transformed by using Cauchy's theorem. Precisely, we apply the Cauchy's theorem to the integral of the integrand appearing in (48) over a closed contour consisting of $\mathbb{R}^+$, the positive part of the imaginary axis shifted by a small positive real number and a quarter of a circle with a very large radius. This last part vanishes as a consequence of the high frequency transparency of the mirrors. The integral over the whole contour also vanishes since the integrand is an analytical function in the domain enclosed by the contour. As a consequence, the integral F_r may be written under the equivalent form F_i ($\varepsilon \to 0^+$)

$$F_r = F_i = \int_\varepsilon^{\varepsilon+\imath\infty} \frac{{\rm d}z}{2\pi c}\;\hbar z\;f[z]\;\coth\frac{\hbar z}{2k_{\rm B}T}\;. \quad (50)$$

The same transformation is then performed for F_r^* which is the integral of the same function over the negative part $\mathbb{R}^-$ of the real axis, run from $-\infty$ to 0. F_r^* is equal to F_i^*, the integral of the same integrand over the positive part of the imaginary axis shifted by a small negative real number $-\varepsilon$ and run from $-\varepsilon-\imath\infty$ to $-\varepsilon$.

In the end, the Casimir force (48) is the integral over a contour which encircles the imaginary axis, and it is thus found to be a discrete sum of the values of the function

$zf[z]$ at the Matsubara poles z_n

$$F = -2k_{\rm B}T \sum_n{}' \frac{\kappa_n r[\imath c\kappa_n] e^{-2\kappa_n L}}{1 - r[\imath c\kappa_n] e^{-2\kappa_n L}} \ ,$$
$$\kappa_n \equiv \frac{\xi_n}{c} = n\kappa_1 \quad , \quad \kappa_1 = \frac{2\pi k_{\rm B}T}{\hbar c} \ . \tag{51}$$

The primed sum symbol implies that the contribution of the zeroth Matsubara pole at $n = 0$ is counted for only one half (symbol written here for a function $\varphi(n)$)

$$\sum_n{}' \varphi(n) \equiv \frac{1}{2}\varphi(0) + \sum_{n=1}^{\infty} \varphi(n) \ . \tag{52}$$

This final expression is always finite for any properly defined model of mirrors.

Limiting cases

In the limit $T \to 0$, the ensemble of Matsubara poles becomes a cut along the imaginary axis (the function $\coth(\hbar z/2k_{\rm B}T)$ thus goes to +1 for $\mathrm{Re}\, z > 0$ and to -1 for $\mathrm{Re}\, z < 0$). The discrete sum (51) is then written as an integral over the positive part of the imaginary axis

$$F_0 = -\frac{\hbar c}{\pi} \int_0^{\infty} \mathrm{d}\kappa \ \frac{\kappa \ r[\imath\xi]}{e^{2\kappa L} - r[\imath\xi]} \quad , \quad \kappa \equiv \frac{\xi}{c} \ . \tag{53}$$

For perfect mirrors, i.e. when r may be taken as unit value at all frequencies contributing to the integral (53), a universal result is obtained, which no longer depends on the specific properties of the mirrors

$$F_0[r \to 1] = -\frac{\hbar c}{\pi} \int_0^{\infty} \mathrm{d}\kappa \ \frac{\kappa}{e^{2\kappa L} - 1} = -\frac{\hbar c \pi}{24 L^2} \ . \tag{54}$$

We have used the fact that the Riemann zeta function

$$\zeta(s) = \frac{1}{\Gamma(s)} \int_0^{\infty} \frac{x^{s-1}}{e^x - 1} \, \mathrm{d}x = \sum_{n=1}^{\infty} \frac{1}{n^s} \ . \tag{55}$$

takes the value $\zeta(2) = \pi^2/6$ for $s = 2$. Other values of the same function will appear in various places in Casimir force calculations with perfectly reflecting mirrors.

For real mirrors the product of reflection amplitudes $r = r_1 r_2$ always has a modulus smaller than unity. It follows that the integral is always regular with a smaller modulus than for perfect mirrors. If the two mirrors are identical ($r_1 = r_2$), then their product r is positive and the force is attractive as in the case of perfect mirrors. The expression of the Casimir force as the integral (54) over imaginary frequencies is convenient to discuss the meaning of the limit of perfect mirrors. Taking as an example the model (30), we indeed see that (53) tends to (54) as soon as the characteristic frequency Ω at which the reflection falls down is larger than the typical frequencies $\omega \sim c/L$ contributing to the integral.

E. The Casimir free energy and phase-shift interpretation

We now write an expression for the Casimir free energy and show that it can be given an interpretation in terms of scattering phase-shifts. We also obtain expressions for the Casimir entropy and Casimir internal energy.

The Casimir free energy

We come back to the expression (48) of the force as an integral over real frequencies and write it as the differential of a free energy $\mathcal{F}$ with respect to L

$$F = -\frac{\partial \mathcal{F}(L,T)}{\partial L} \ ,$$
$$\mathcal{F} = \int_0^{\infty} \frac{\mathrm{d}\omega}{2\pi} \left(1 + 2\overline{n}_{\omega}\right) \frac{\hbar}{2\imath} \ln \frac{d}{d^*} \ , \tag{56}$$
$$d \equiv 1 - r e^{2ikL} \ .$$

We show in the following that this formula can be given a nice interpretation in terms of phase-shifts [28]. Note that, though $\mathcal{F}$ could be changed by a $L-$independent contribution without changing the result for F, the form of $\mathcal{F}$ given in (56) is fixed by the phase-shift interpretation discussed below.

The phase-shift interpretation

To the aim of introducing the phase-shift interpretation, we put the cavity of Figure 7 inside a quantization box with a much larger size $\mathcal{L} \gg L$ and periodic conditions, as sketched on Figure 8.

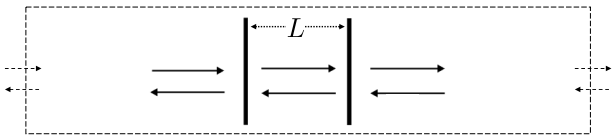

FIG. 8. The scattering system, a cavity of length L, is put in a much larger quantization box, and the Casimir effect is calculated as the change of free energy of the large box.

In the absence of the scatterer, the modes in the large box would have their wavelengths determined by the box size through $k_n^{\pm}\mathcal{L} = 2n\pi$, where $\pm$ labels the rightward and leftward propagation directions which correspond to degenerate solutions. The eigen-modes in the presence of the scatterer are thus determined by the eigenvalues $e^{\imath\delta_n^{\pm}}$ of the unitary $S-$matrix through $k_n^{\pm}\mathcal{L} + \delta_n^{\pm} = 2n\pi$. The change of global energy of the modes at a given frequency ω is then determined by the quantity $-\hbar c\,(\delta_n^+ + \delta_n^-)$ proportional to the sum of the two phase-shifts at this frequency. As a consequence, we do not need to solve

the full eigenvalue problem for the $S-$matrix, but we need only to calculate the logarithm of its determinant $\ln\det S = \imath\,(\delta_n^+ + \delta_n^-)$.

The relation between the expression (56) of the free energy and the phase-shift interpretation is then fixed by noting that the expression (37) written above for the $S-$matrix associated to the cavity leads to the following relation between the determinants

$$\det S_{12} = (\det S_1)\,(\det S_2)\ \frac{d^*}{d}\ . \tag{57}$$

where we have denoted S_{12} the scattering matrix for the compound system consisting of the two mirrors 1 and 2 (it was simply denoted S in (37)). One thus deduces

$$\ln\det S_{12} = \ln\det S_1 + \ln\det S_2 + \ln\frac{d^*}{d}\ . \tag{58}$$

It is now clear that the Casimir free energy (56) is given by a difference between changes of free energies $\Delta\mathcal{F}$ calculated in three different scattering configurations

$$\mathcal{F} = \Delta\mathcal{F}_{12} - \Delta\mathcal{F}_1 - \Delta\mathcal{F}_2\ , \tag{59}$$

with each of these quantities determined by the phase-shifts for the associated $S-$matrix

$$\Delta\mathcal{F}_{12} = \int_0^\infty \frac{\mathrm{d}\omega}{2\pi}\,(1+2\overline{n}_\omega)\,\frac{\imath\hbar}{2}\ln\left(\det S_{12}\right)\ . \tag{60}$$

Similar expressions hold for the change of free energies $\Delta\mathcal{F}_1$ and $\Delta\mathcal{F}_2$ associated respectively with mirrors 1 and 2 placed in the large box on Figure 8.

In fact, each of the changes is itself a difference of free energies calculated in the presence and in the absence of the scatterer

$$\Delta\mathcal{F}_{12} \equiv \mathcal{F}_{12} - \mathcal{F}_0\ ,\ \Delta\mathcal{F}_i \equiv \mathcal{F}_i - \mathcal{F}_0\ ,\ i=1,2\ , \tag{61}$$

with the subscript 0 labeling the configuration with no scatterer. In the end, the Casimir free energy is a difference involving four different configurations

$$\begin{aligned}\mathcal{F} &= (\mathcal{F}_{12}-\mathcal{F}_0) - (\mathcal{F}_1-\mathcal{F}_0) - (\mathcal{F}_2-\mathcal{F}_0)\\ &= \mathcal{F}_{12} - \mathcal{F}_1 - \mathcal{F}_2 + \mathcal{F}_0\ .\end{aligned} \tag{62}$$

It is worth emphasizing at this point that the definitions of $\mathcal{F}_{12}$, $\mathcal{F}_1$, $\mathcal{F}_2$ and $\mathcal{F}_0$ are affected by the problem of vacuum energy discussed above. Meanwhile $\Delta\mathcal{F}_{12}$, $\Delta\mathcal{F}_1$ and $\Delta\mathcal{F}_2$ are self-energies, and their proper evaluation should involve some renormalization procedure. In contrast, the Casimir free energy is always a finite quantity, the evaluation of which does not require renormalization [28].

Casimir thermodynamics

We can then write other thermodynamical functions associated with the Casimir effect. One may in particular define an entropy $\mathcal{S}$ from the free energy $\mathcal{F}$

$$\mathcal{S} = -\frac{\partial\mathcal{F}(L,T)}{\partial T}\ , \tag{63}$$

and then an internal energy $\mathcal{E}$

$$\mathcal{E} = \mathcal{F} + T\mathcal{S} = \mathcal{F} - T\frac{\partial\mathcal{F}(L,T)}{\partial T}\ . \tag{64}$$

These thermodynamical functions obey the usual thermodynamical relations such as

$$\mathrm{d}\mathcal{F} = -F\mathrm{d}L - \mathcal{S}\mathrm{d}T\quad ,\quad \mathrm{d}\mathcal{E} = -F\mathrm{d}L + T\mathrm{d}\mathcal{S}\ . \tag{65}$$

The last relation just means that the change $\mathrm{d}\mathcal{E}$ of internal energy under a transformation is the sum of a mechanical work $-F\mathrm{d}L$ and of a heat term $T\mathrm{d}\mathcal{S}$.

These thermodynamical functions can be deduced from the free energy $\mathcal{F}(L,T)$ written previously as an integral over real frequencies or, equivalently, from its form as a Matsubara sum

$$\mathcal{F}(L,T) = k_{\mathrm{B}}T{\sum_n}'\ln d[\imath\xi_n]\ . \tag{66}$$

This expression can be obtained from (56) by using anew the Cauchy's theorem. Equivalently, it can be obtained from the Casimir force (51) written above as a sum over Matsubara poles.

III. THE CASIMIR FORCE IN 3-DIMENSIONAL SPACE

We come now to the last section of these lecture notes, which is devoted to the discussion of the Casimir force in three-dimensional (3d) space.

We will mainly discuss the geometry of two plane and parallel mirrors, described by specular scattering amplitudes. This case constitutes a trivial extension of the derivation in 1d space though a few points have to be treated with greater care. As for the 1d case, we will write a formula valid and regular at thermal equilibrium at any temperature and for any optical model of mirrors obeying causality and high frequency transparency properties [28]. It reproduces the Casimir ideal formula in the limits of perfect reflection and null temperature, but can also be used for calculating the Casimir force between arbitrary mirrors, as soon as the reflection amplitudes are specified. For mirrors characterized by Fresnel reflection amplitudes deduced from a linear and local dielectric function, the Scattering Formalism leads to the same results as the Lifshitz's method [31–33].

The section ends with a short presentation of the general scattering formalism which allows one to deal with non specular reflection and arbitrary geometries [37].

A. Free electromagnetic fields in 3d space

Modes for electromagnetic fields

The free modes for electromagnetic fields in 3d space are the free solutions of Maxwell equations in vacuum.

They correspond to frequency and wave-vector related through the dispersion relation

$$\frac{\omega^2}{c^2} = k_x^2 + k_y^2 + k_z^2 = \mathbf{k}^2 + k_z^2 \quad , \quad \mathbf{k}^2 \equiv k_x^2 + k_y^2 \ . \quad (67)$$

As mirrors will be specified later on to have their surfaces parallel to the (x, y) plane, k_z is the longitudinal part of the wave-vector and $\mathbf{k} \equiv (k - x, k_y)$ its transverse part. We introduce a direction of propagation as in 1d calculations : $\eta = +1$ corresponds to rightward propagation and $\eta = -1$ to leftward propagation. η is the sign of k_z ($\eta = \mathrm{sign}\,(k_z) = \mathrm{sign}\,(\cos\theta)$) and it appears in the expression of k_z in terms of frequency and transverse wave-vector $k_z = \eta\sqrt{\frac{\omega^2}{c^2} - \mathbf{k}^2}$.

The propagation direction is defined by the incidence angle θ and azimuth φ

$$k = \frac{\omega}{c}\widehat{k} \quad , \quad \widehat{k} = \begin{pmatrix} \widehat{k}_x \\ \widehat{k}_y \\ \widehat{k}_z \end{pmatrix} = \begin{pmatrix} \sin\theta\cos\varphi \\ \sin\theta\sin\varphi \\ \cos\theta \end{pmatrix} \ . \quad (68)$$

Unit wave-vector and polarization vectors for electric ($\widehat{\alpha}$) and magnetic ($\widehat{\beta}$) fields form an ortho-normal basis for each polarization p =TE,TM with $\widehat{\beta}^p = \widehat{k} \times \widehat{\alpha}^p$ in each case

$$\widehat{\alpha}^{\mathrm{TE}} = \widehat{\beta}^{\mathrm{TM}} = \begin{pmatrix} -\sin\varphi \\ \cos\varphi \\ 0 \end{pmatrix} \ ,$$
$$\widehat{\alpha}^{\mathrm{TM}} = -\widehat{\beta}^{\mathrm{TE}} = \begin{pmatrix} \cos\theta\cos\varphi \\ \cos\theta\sin\varphi \\ -\sin\theta \end{pmatrix} \ . \quad (69)$$

Electric and magnetic fields

Electric and magnetic fields are then obtained as linear superpositions of modes labeled by m and η

$$E = \sum_{m,\eta}\sqrt{\frac{\hbar\omega}{2\varepsilon_0}}\widehat{\alpha}_{m,\eta}\big(-\imath a_{m,\eta}e^{-\imath\omega t+\imath\mathbf{kr}+\imath k_z z} + \imath a^\dagger_{m,\eta}e^{\imath\omega t-\imath\mathbf{kr}-\imath k_z z}\big) \ ,$$
$$B = \sum_{m,\eta}\sqrt{\frac{\hbar\omega\mu_0}{2}}\widehat{\beta}_{m,\eta}\big(-\imath a_{m,\eta}e^{-\imath\omega t+\imath\mathbf{kr}+\imath k_z z} + \imath a^\dagger_{m,\eta}e^{\imath\omega t-\imath\mathbf{kr}-\imath k_z z}\big) \ . \quad (70)$$

m gathers all quantum numbers but η and can be written under two alternative forms

$$m \equiv (\mathbf{k}, |k_z|, p) \quad \text{or} \quad m \equiv (\mathbf{k}, \omega, p) \ . \quad (71)$$

η is treated separately because the two modes $\eta = \pm 1$ corresponding to the same m will be coupled by the scattering processes studied later on. The sum over modes has the following definition (A is an area introduced for defining integrals over $\mathbf{k}$)

$$\sum_m \equiv \sum_p \iint \frac{A\mathrm{d}^2\mathbf{k}}{4\pi^2}\int\frac{\mathrm{d}|k_z|}{2\pi} = \sum_p \iint \frac{A\mathrm{d}^2\mathbf{k}}{4\pi^2}\int\frac{\omega\mathrm{d}\omega}{2\pi c^2|k_z|} \ . \quad (72)$$

Finally, the symbols $a_{m,\eta}$ and $a^\dagger_{m,\eta}$ appearing in the positive and negative frequency components are the annihilation and creation operators of quantum electrodynamics [169]. Their commutation relations and correlations are immediate generalizations of the ones (21) and (25) written for 1d calculations.

Note that we have used the electromagnetic constants in vacuum ε_0 and μ_0. In the following, the symbol ε will be used as a relative permittivity with its value in vacuum being unity and the relative permittivity will keep its unit value in vacuum.

Energy density and radiation pressure

Energy-momentum densities and radiation pressures are components of the Maxwell stress tensor [3]. In particular, the energy per unit volume e is the component T_{00}

$$e = \frac{\varepsilon_0\ E^{\mathrm{T}}E}{2} + \frac{B^{\mathrm{T}}B}{2\mu_0} \ , \quad (73)$$

where T symbolizes a matrix transposition. Substituting the expression of free fields and calculating the mean value of energy density in a thermal state, we obtain a simple generalization of the expression (26) written for 1d calculations.

$$\langle\, e\,(u)\,\rangle_{\mathrm{therm}} = \sum_{m,\eta}\frac{\hbar\omega_m}{2}\left(1 + 2\overline{n}_m\right) \ . \quad (74)$$

We come then to the radiation pressure on plane mirrors parallel to the (x, y) plane which corresponds to the component T_{zz} of the Maxwell stress tensor

$$\frac{\varepsilon_0\left(E_xE_x + E_yE_y - E_zE_z\right)}{2} + \frac{B_xB_x + B_yB_y - B_zB_z}{2\mu_0} \ . \quad (75)$$

The quantum average of this quantity in a thermal state leads to

$$\sum_{m,\eta}\frac{\hbar\omega_m}{2}\cos^2\theta_m\left(1 + 2\overline{n}_m\right) \ . \quad (76)$$

The sums over modes written in the preceding expressions are infinite but the force on mirrors will be obtained as a finite difference between the radiation pressure acting on their two sides.

B. Scattering on plane mirrors in 3d space

We consider plane mirrors parallel to the (x, y) plane, that is also surfaces of constant z in 3d space. Scattering on such mirrors is a simple extension of that described in the 1d case because of symmetry considerations. Invariance under time translations and lateral space translations implies that the frequency frequency ω, transverse wave-vector $\mathbf{k}$ and polarization p are preserved. The scattering process is *specular* and it only affects the parameter η. We first consider lossless mirrors and then address the problem of losses.

A lossless mirror in 3d space

This specular scattering on a lossless mirror is schematically represented on Figure 9. On the left part, the angles of incidence are shown for the input and output fields. On the right part in contrast, they are only implicit. It thus follows that the sketch of the scattering process is alike that drawn on Figure 5 for the 1d case.

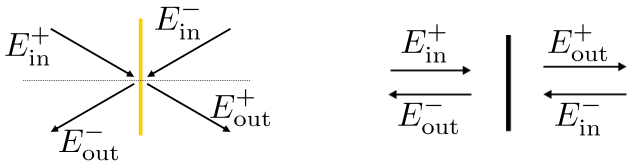

FIG. 9. Schematic representation of specular scattering upon a lossless mirror in 3d space, with angles of incidence explicitly shown on the left part but only implicit on the right part.

As in the 1d case, the scattering matrix is just a 2×2 matrix giving the two output fields in terms of the two input ones

$$\begin{pmatrix} E^+_{\rm out} \\ E^-_{\rm out} \end{pmatrix} = S_1 \begin{pmatrix} E^+_{\rm in} \\ E^-_{\rm in} \end{pmatrix} ,$$
$$S_1[m] = \begin{pmatrix} t_1[m] & r_1[m] e^{-2\imath |k_z| q_1} \\ r_1[m] e^{2\imath |k_z| q_1} & t_1[m] \end{pmatrix} . \quad (77)$$

Scattering amplitudes have been written as in (28) : r_1 and t_1 are defined for a mirror located at $x = 0$ and depend on the quantum number m for real mirrors ; the general case is then described by phases determined by the position q_1 of the mirror and the longitudinal wave-vector k_z.

A lossless cavity in 3d space

The specular scattering on a cavity made of two mirrors is schematically represented on Figure 10.

Most calculations are the same as for the 1d case, with the effect of the cavity described by a global scattering matrix and a resonance matrix as in (36)

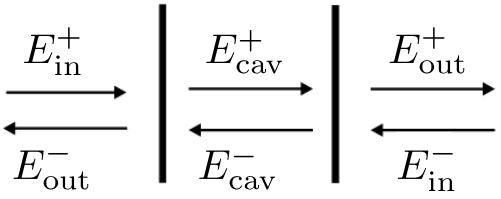

FIG. 10. Schematic representation of specular scattering upon a cavity in 3d space, with the same convention as on the right part of Figure 9.

$$\begin{pmatrix} E^+_{\rm out} \\ E^-_{\rm out} \end{pmatrix} = S \begin{pmatrix} E^+_{\rm in} \\ E^-_{\rm in} \end{pmatrix} ,$$
$$\begin{pmatrix} E^+_{\rm cav} \\ E^-_{\rm cav} \end{pmatrix} = R \begin{pmatrix} E^+_{\rm in} \\ E^-_{\rm in} \end{pmatrix} . \quad (78)$$

The matrices S and R are obtained from the scattering amplitudes associated with the mirrors 1 and 2 as in the 1d case, that is to say from equations (37) and (40) with the phase factors $e^{\pm \imath k L}$ replaced by $e^{\pm \imath |k_z| L}$.

As the global $S-$matrix is unitary, radiation pressures on the outer sides of the mirrors are given by the expression (76). Meanwhile, radiation pressures on the inner sides of the mirrors are modified by a factor given by the common value of the diagonal elements in $RR^\dagger$

$$g_m \equiv 1 + f_m + f_m^* = \frac{1 - |r_m|^2}{|1 - r_m e^{2\imath |k_z| L}|^2} ,$$
$$f_m \equiv \frac{r_m e^{2\imath |k_z| L}}{1 - r_m e^{2\imath |k_z| L}} . \quad (79)$$

The effective pressure on the mirror is then given by the difference between the pressures on its two sides

$$\frac{1}{A} \sum_m \hbar \omega_m \cos^2 \theta_m \, (1 + 2\overline{n}_m) \, (g_m - 1)$$
$$= \frac{1}{A} \sum_m \hbar \omega_m \cos^2 \theta_m \, (1 + 2\overline{n}_m) \, (f_m + f_m^*) . \quad (80)$$

The left-hand side corresponds to the radiation pressure interpretation already discussed in the 1d case while the right-hand side, written in terms of the causal function f, is the basis for transformations using the Cauchy's theorem. However, some elements are now to be treated with more care before the Casimir pressure is obtained.

C. The Casimir pressure between two plates in 3d space

We now extend the derivations to take into account two effects which play an important role for calculations in 3d space. First, we want to discuss the effect of dissipation inside the mirror and the associated fluctuations. Then, we address the contributions of evanescent waves

which have to be added to that of ordinary propagation waves [30].

Generalization for lossy mirrors

As already explained, the mirrors used in the experiments are made of metals and they have losses associated to the dissipation inside the matter. As a consequence, the scattering matrices defined above cannot be considered as unitarity. In other words, there are additional fluctuations accompanying losses which should be taken into account in a large scattering matrix described the coupling of the modes of interest and the noise modes [170–172].

At this point, it is worth using a theorem which gives the commutators of the intra-cavity fields as the product of those well known for fields outside the cavity and the factors g_m introduced in (79). This theorem, which was demonstrated with an increasing range of validity in [28, 30, 171], proves that the expression written in (79) for lossless mirrors is still true for lossy mirrors. We then assume thermal equilibrium for the whole system, which means that input fields as well as fluctuations associated with electrons, phonons and any loss mechanism inside the mirrors have to correspond to the same temperature T, whatever their microscopic origin may be. Then, the radiation pressures are given by the expressions written above and the last equation becomes the Casimir pressure, valid for lossy as well as lossless mirrors,

$$P = \frac{1}{A}\sum_m \hbar\omega_m \cos^2\theta_m \,(1+2\overline{n}_m)\,(f_m + f_m^*) \ . \quad (81)$$

Generalization for evanescent waves

Up to now, we have discussed the contributions of ordinary waves freely propagating outside and inside the cavity, which correspond to real wave-vectors with k_z real, that is also $\omega > c|\mathbf{k}|$. Equation (81) thus reflects the intuitive picture of radiation pressure of vacuum and thermal fluctuations, as discussed above in the 1d case. In the 3d case, we have also to take into account the contribution of evanescent waves (see §1.5.4 in [173]), which correspond to imaginary values of k_z, that is also frequencies in the interval $0 < \omega < c|\mathbf{k}|$.

Those waves propagate inside the mirrors with an incidence angle larger than the limit angle and they also exert a radiation pressure on the mirrors, due to the frustrated reflection phenomenon. In fact, the expression (81) of the Casimir pressure has to be understood as including these contributions [30]. They are obtained through an analytical continuation of those of ordinary waves, using the well defined analytic behavior of the causal function f_m. This analytical continuation has to be defined for fixed values of the lateral wave-vector $\mathbf{k}$ and polarization p.

Using the definition (72) of the sum over modes and the relation $\cos\theta = ck_z/\omega$, one finally gets the Casimir pressure (81) as the real part of an integral over the positive part $\mathbb{R}^+$ of the real axis (to be compared with (48))

$$P = P_r + P_r^* \ , \quad (82)$$
$$P_r \equiv \sum_p \iint \frac{\mathrm{d}^2\mathbf{k}}{4\pi^2}\int_0^\infty \frac{\mathrm{d}\omega}{2\pi}\hbar|k_z| f_m \ \coth\frac{\hbar\omega}{2k_{\mathrm{B}}T} \ .$$

We stress again that the integral over $\mathbb{R}^+$ includes the contributions of evanescent waves $0 < \omega < c|\mathbf{k}|$ besides those of ordinary waves $c|\mathbf{k}| < \omega$.

Casimir pressure as an integral over imaginary frequencies

One now transforms the expression (82) of the Casimir pressure by using Cauchy's theorem as in the 1d case. In the end of the derivation, the Casimir pressure is the integral over a contour which encircles the imaginary axis, and it is thus found to be a discrete sum of the values of the function $|k_z| f_m$ at the Matsubara poles

$$P = -k_{\mathrm{B}}T\sum_p \int \frac{\mathrm{d}^2\mathbf{k}}{(2\pi)^2}\,{\sum_n}' \frac{2\kappa_n\, r_{\mathbf{k}}^p[i\xi_n]e^{-2\kappa_n L}}{1 - r_{\mathbf{k}}^p[i\xi_n]e^{-2\kappa_n L}} \ , \quad (83)$$

where κ is obtained from $|k_z|$ through an analytical continuation for imaginary frequencies $\omega_n = i\xi_n$

$$\kappa_n = \sqrt{\mathbf{k}^2 + \frac{\xi_n^2}{c^2}} \quad , \quad \xi_n = n\frac{2\pi k_{\mathrm{B}}T}{\hbar} \ . \quad (84)$$

As in the 1d case, this expression is finite for any properly defined model of mirrors.

Zero temperature limit

In the limit $T \to 0$, the ensemble of Matsubara poles becomes a cut along the imaginary axis and the Matsubara sum (83) becomes an integral over the positive part of the imaginary axis ($P_0 \equiv P_{T=0}$)

$$P_0 = -2\sum_p \iint \frac{\mathrm{d}^2\mathbf{k}}{4\pi^2}\int_0^\infty \frac{\mathrm{d}\xi}{2\pi}\hbar\kappa \frac{r_{\mathbf{k}}^p[i\xi]e^{-2\kappa L}}{1 - r_{\mathbf{k}}^p[i\xi]e^{-2\kappa L}} \ ,$$
$$\kappa = \sqrt{\mathbf{k}^2 + \frac{\xi^2}{c^2}} \ . \quad (85)$$

For perfect mirrors, i.e. when r may be taken as unit value at all frequencies contributing to the integral (85), a universal result is obtained, which no longer depends on the specific properties of the mirrors

$$P_0[r \to 1] = -\frac{\hbar c}{\pi^2}\int_0^\infty \frac{\kappa^3 \mathrm{d}\kappa}{e^{2\kappa L} - 1} = -\frac{\hbar c\pi^2}{240 L^4} \ . \quad (86)$$

We have used the fact that the Riemann zeta function (55) takes the value $\zeta(4) = \pi^4/90$ for $s = 4$.

D. Models for metallic mirrors

We now come back to the discussion presented in section I for the models of metallic mirrors used in the experiments. The common model is that of bulk mirrors, in fact thick slabs, made with metals for example gold. The optical response of the metal is described by a local dielectric response function and the reflection amplitudes on each mirror then deduced by using Fresnel laws.

Fresnel reflection amplitudes

Reflection amplitudes on a thick slab described by a local dielectric response ε are given by the well known Fresnel laws for the TE and TM polarizations (see §1.5.1 in [173] or §86 in [174])

$$r_1^{\rm TE}[\omega] = \frac{k_z - K_z}{k_z + K_z} \quad , \quad r_1^{\rm TM}[\omega] = \frac{K_z - \varepsilon k_z}{K_z + \varepsilon k_z} \ , \quad (87)$$

where K_z and k_z are the longitudinal wave-vectors in matter and vacuum respectively

$$K_z = \sqrt{\varepsilon \frac{\omega^2}{c^2} - \mathbf{k}^2} \quad , \quad k_z = \sqrt{\frac{\omega^2}{c^2} - \mathbf{k}^2} \ . \quad (88)$$

When the frequency is continued to imaginary values, these expressions become

$$r_1^{\rm TE}[i\xi] = \frac{\kappa - K}{\kappa + K} \quad , \quad r_1^{\rm TM}[i\xi] = \frac{K - \varepsilon[i\xi]\kappa}{K + \varepsilon[i\xi]\kappa} \ ,$$
$$K = \sqrt{\varepsilon[i\xi]\frac{\xi^2}{c^2} + k^2} \quad , \quad \kappa = \sqrt{\frac{\xi^2}{c^2} + k^2} \ . \quad (89)$$

When the reflection amplitudes (89) are inserted in the expression (83) of the pressure, the formula obtained in 1956 by E.M. Lifshitz [31] and derived again in 1961 by I.E. Dzyaloshinskii, E.M. Lifshitz and L.P. Pitaevskii [32] is recovered (see also Chap. VIII in [33]). We may stress at this point that this formula was obtained through a different derivation, with all fluctuations originating from matter. In fact this expression was written in terms of the dielectric function and not of reflection amplitudes. To our best knowledge, Kats was the first to notice that it could be written in terms of the reflection amplitudes [175]. We may quote at this point a few alternative derivations of this formula through different methods [176–184].

We may remark that the optical response of the bulk material cannot always be described by a local dielectric function. In this case, the description in terms of reflection amplitudes is still valid, though the reflection amplitudes cannot be written under the specific forms (89). More detailed descriptions can for example be determined from microscopic models of metallic conduction. Attempts in this direction and discussions can be found for example in [116–122].

Models for dielectric functions

As already discussed in section I, the dielectric function ε is usually obtained from optical data [29, 73]. These data are then extrapolated at low frequencies by using the dissipative Drude model (9) for the conductivity of the metal [75]. In contrast to the plasma model (11) which corresponds to the lossless limit $\gamma = 0$, the dissipative Drude model meets the well-known fact that gold has a finite static conductivity (10).

The two models lead to different predictions for the Casimir pressure, in particular at the limits of large distances or large temperatures. This can be attributed to different limiting cases at zero frequency. The Drude model indeed corresponds to

$$\lim_{\omega\to 0} r_{\mathbf{k}}^{\rm TE}[\omega] = 0 \ , \ \lim_{\omega\to 0} r_{\mathbf{k}}^{\rm TM}[\omega] = 1 \ , \ \gamma \neq 0 \ , \quad (90)$$

whereas the plasma model leads to

$$\lim_{\omega\to 0} r_{\mathbf{k}}^{\rm TE}[\omega] = 1 \ , \ \lim_{\omega\to 0} r_{\mathbf{k}}^{\rm TM}[\omega] = 1 \ , \ \gamma = 0 \ . \quad (91)$$

High temperature limit

At the limit of high temperatures $\kappa_1 L \gg 1$, the Matsubara poles with $n > 0$ give an exponentially small contribution to the Casimir pressure (83). The result is thus dominated by the contribution of the zeroth pole $n = 0$ ($P_\infty \equiv P_{T\to\infty}$)

$$P_\infty = -k_{\rm B}T \sum_p \int \frac{{\rm d}^2\mathbf{k}}{(2\pi)^2} \frac{|\mathbf{k}| r_{\mathbf{k}}^p[0] e^{-2|\mathbf{k}|L}}{1 - r_{\mathbf{k}}^p[0] e^{-2|\mathbf{k}|L}} \ . \quad (92)$$

It follows that the asymptotic Casimir pressure (92) has different values for a dissipative model

$$P_\infty = -\frac{k_{\rm B}T}{2\pi} \int_0^\infty \frac{k^2\,{\rm d}k}{e^{2kL} - 1} = -\frac{k_{\rm B}T}{8\pi L^3}\zeta(3) \ , \ \gamma \neq 0 \quad (93)$$

and a lossless model

$$P_\infty = -\frac{k_{\rm B}T}{\pi} \int_0^\infty \frac{k^2\,{\rm d}k}{e^{2kL} - 1} = -\frac{k_{\rm B}T}{4\pi L^3}\zeta(3) \ , \ \gamma = 0 \quad (94)$$

$\zeta(3) \simeq 1.202$ is the value of the Riemann zeta function (55) for $s = 3$. As already discussed in section I, there is a large factor 2 between the two predictions because the two polarizations contribute equally for the plasma model, as well as for perfect mirrors, whereas only one polarization contributes for the Drude model.

E. The Casimir free energy in 3d space

Using the results already obtained in the 1d case, we write an expression for the Casimir free energy and show that it can be given an interpretation in terms of scattering phase-shifts. We also obtain expressions for the Casimir entropy and Casimir internal energy.

The Casimir free energy and phase-shift interpretation

The expression (82) of the Casimir pressure can be written as the differential $P = -\partial\mathcal{F}/\partial V$ of a free energy $\mathcal{F}(V,T)$ with respect to the volume $V \equiv AL$

$$\mathcal{F} = \sum_p A \iint \frac{\mathrm{d}^2\mathbf{k}}{4\pi^2} \int_0^\infty \frac{\mathrm{d}\omega}{2\pi} (1 + 2\overline{n}_\omega) \times \frac{\hbar}{2i} \ln \frac{1 - re^{2i|k_z|L}}{1 - r^* e^{-2i|k_z|L}} \ . \quad (95)$$

The interpretation of this formula in terms of phase-shifts is the same as in the 1d case [28] and we do not repeat here the derivation presented in section II. In the end of this derivation, the Casimir free energy (95) is given by a difference (59) of changes of free energies calculated in three different scattering configurations, with each of these quantities determined by an integral (60) over all modes. As already emphasized, the Casimir free energy is always a finite quantity, the evaluation of which does not require a renormalization [28].

Casimir thermodynamics

We can then write other thermodynamical functions associated with the Casimir effect. One may in particular define an entropy $\mathcal{S} - \partial\mathcal{F}/\partial T$ and then an internal energy $\mathcal{E} = \mathcal{F} + T\mathcal{S}$. These thermodynamical functions obey the usual thermodynamical relations ($V \equiv AL$)

$$\mathrm{d}\mathcal{F} = -P\mathrm{d}V - \mathcal{S}\mathrm{d}T \quad , \quad \mathrm{d}\mathcal{E} = -P\mathrm{d}V + T\mathrm{d}\mathcal{S} \ . \quad (96)$$

These thermodynamical functions can be deduced from the free energy (95) written previously as an integral over real frequencies or, equivalently, from its form as a Matsubara sum

$$\mathcal{F} = k_\mathrm{B}T \sum_n{}' \mathrm{Tr} \ln d[i\xi_n] \ . \quad (97)$$

We have used the denominator of the $S-$matrix to write the free energy

$$d^p_\mathbf{k}[i\xi_n] = 1 - r^p_\mathbf{k}[i\xi_n] e^{-2\kappa_n L} \ , \ \kappa_n = \sqrt{\frac{\xi_n^2}{c^2} + k^2} \ , \quad (98)$$

and we have also introduced a trace over polarizations and transverse wave-vectors in order to simplify the expression

$$\mathrm{Tr}\, d \equiv \sum_p \int \frac{A\mathrm{d}^2\mathbf{k}}{(2\pi)^2} \ d^p_\mathbf{k} \ . \quad (99)$$

The expression (97) for the free energy is completely equivalent to the expression (83) written above for the pressure.

F. General scattering formula

We now present a more general scattering formula allowing one to calculate the Casimir force between stationary disjoint objects with arbitrary shapes. We also review rapidly some of the applications of this new method which have been dedicated in the recent years to the study of non trivial geometries. More exhaustive reviews of the topic can be found in [34–39].

The non-specular scattering formula

We consider a geometrical configuration with two disjoint scatterers at rest in electromagnetic vacuum. The scattering matrix is now a large matrix which accounts for non-specular reflection mixing different wave-vectors and polarizations while preserving frequency if the scatterers are at rest. Of course, the non-specular scattering formula is the generic one while specular reflection is an idealization for perfectly plane and flat plates.

The reasoning presented above leads to an expression of the Casimir free energy as the sum of all phase-shifts contained in the large $S-$matrix [34]. Causality and high-frequency transparency then allow one to write it as a Matsubara sum (to be compared with (97))

$$\mathcal{F} = k_\mathrm{B}T \sum_m{}' \mathrm{Tr} \ln \mathcal{D}(i\xi_m) \ , \quad \xi_m \equiv \frac{2\pi m k_\mathrm{B} T}{\hbar} \ . \quad (100)$$

Each term in this sum is the trace of a large matrix which describes all couplings at a given frequency. The matrix $\mathcal{D}$ (here written at Matsubara frequencies $\omega_m = i\xi_m$) is the denominator of the scattering matrix. It describes the resonance properties of the cavity formed by the two objects (to be compared with (98))

$$\mathcal{D} = 1 - \mathcal{R}_1 e^{-\mathcal{K}L} \mathcal{R}_2 e^{-\mathcal{K}L} \ . \quad (101)$$

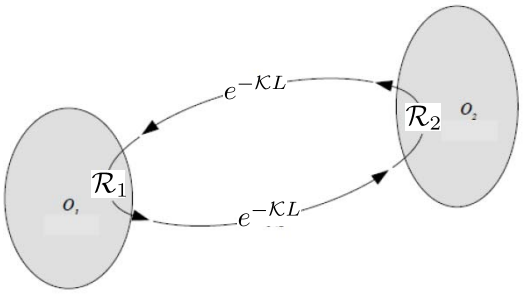

FIG. 11. General scattering configuration with two objects O_1 and O_2 in vacuum : the Casimir free energy can be calculated from the denominator (101) describing the resonance properties of the cavity formed by the two objects and given by the reflection matrices $\mathcal{R}_1$ and $\mathcal{R}_2$ and the propagation matrices $e^{-\mathcal{K}L}$.

The matrices $\mathcal{R}_1$ and $\mathcal{R}_2$ represent reflection on the two objects 1 and 2 respectively while $e^{-\mathcal{K}L}$ describes propagation. Note that the matrices $\mathcal{D}$, $\mathcal{R}_1$ and $\mathcal{R}_2$, which

were diagonal in the plane wave basis for specular scattering, are no longer diagonal in the general case of non specular scattering. The propagation factors remain diagonal in this basis with their eigenvalues κ written as in (98). Note that the expression (100) does not depend on the choice of a specific basis.

Applications to non trivial geometries

The fact that geometry plays a non trivial role in the context of vacuum energy and Casimir forces has been noticed for a long time [185, 186]. In the plane-sphere geometry for example, the *Proximity Force Approximation* (PFA) can only be valid when the radius is much larger than the separation [187–189]. Recently, calculations have used the general non-specular scattering formula in order to push the theory beyond the PFA and thus open roads to a new domain [34–39].

The first application of the non-specular scattering formula to calculations beyond the PFA was developed in [124, 125] to study the roughness correction to the Casimir force between two planes, in a perturbative expansion with respect to the roughness amplitude. Another geometry studied with this method is that of surfaces with periodic corrugations. As lateral translation symmetry is broken, the Casimir force contains a lateral component which is smaller than the normal one, but has nevertheless been measured in dedicated experiments [190]. Calculations beyond the PFA have first been performed with the simplifying assumptions of perfect reflection [191] or shallow corrugations [192, 193]. As could be expected, the PFA was found to be accurate only in the limit of large corrugation wavelengths.

In recent years, experiments have been able to probe the beyond-PFA regime [194–196]. Exact calculations of the forces between real mirrors with deep corrugations have been performed [197, 198] and comparisons between theory and experiments presented [199, 200]. The same kind of calculations was performed for studying the Casimir torque which appears between two corrugated surfaces with non aligned corrugations [201].

The plane-sphere geometry

Another important application corresponds to the plane-sphere geometry used in most Casimir force experiments and for which explicit *exact calculations* (see a discussion of the meaning of this expression below) have recently been developed (see discussions of the various methods devoted to this problem in [202–206]).

Indeed, exact multipolar expansions have been written for the force in the plane-sphere geometry [207, 208]. These calculations have now been performed for metallic surfaces coupled to electromagnetic vacuum, at zero [209] or non zero temperature [210, 211], and this has opened the way to a comparison with theory of the only experimental study devoted to a test of PFA in the plane-sphere geometry [212]. The results of these calculations is often presented in terms of a ratio ρ of the exact result to the PFA approximation, which is close to unity when the aspect ratio $x \equiv L/R$ is small. An alternative representation is in terms of the *slope* β defined by $\rho \equiv 1 + x\beta$.

In fact, the *exact result* is an infinite series corresponding to a multipolar expansion over the numbers (ℓ, m) which label the basis of spherical waves (with $|m| \leq \ell$). Sums have to be truncated for the numerics to $\ell \leq \ell_{\max}$ and the precision is thus limited for small values of the aspect ratio. The minimum aspect ratio for precise calculations scales as the inverse of the maximum multipolar index $\ell_{\max}$. For some time, extrapolations at low values of x were used to obtain bounds useful for the values of experimental interest. Such a procedure used the idea that the slope β could be represented as a Taylor expansion of the aspect ratio [213–215]. However this idea was finally shown to be wrong in the high temperature limit which corresponds to a classical Casimir effect with an entropic origin [216, 217]. As a consequence, the question of accurate evaluations for the deviation from PFA remains open.

Nano-spheres and atoms close to surfaces

We will end up this paper by considering another case of interest, that of dielectric nano-spheres above a plane, which tends at the limit of a very small sphere to the Casimir-Polder problem.

The calculations easier for nano-spheres than for large spheres because a small number of multipoles is sufficient for reaching a good accuracy. An example of such calculations is given in [218] for nano-diamonds above a copper plate. Of course, the Casimir-Polder expression between an atom and a plane is recovered in the limit of large distances $R \gg L$ where the dipole approximation is sufficient. The Casimir-Polder limit is written in terms of a polarizability for the atom (expression given in [219]). The polarizability of a small sphere is that of a large atom as it is proportional to the volume of the sphere [218].

Conclusion

The general scattering formula allows one to describe all long-range interactions in a unified manner as the change of vacuum energy due to the presence of scatterers in vacuum. Atoms as well as mirrors are completely characterized by scattering amplitudes which have of course different properties. In particular, atomic scattering is weak so that perturbation theory is in general sufficient whereas scattering by mirrors may be saturated (up to 100% reflection). Atoms are local probes of vacuum whereas mirrors are not.

The same general scattering formula thus allows one to treat different cases which lead to a variety of phenomena [34], for example atom/atom, atom/plate or plate/plate interactions, with plane or spherical plates as well as nano-structured surfaces. In order to quote a few examples, it has been possible to study the Casimir-Polder forces or torques for atoms near corrugated surfaces [220–222].

Acknowledgments

The authors thank R.O. Behunin, A. Canaguier-Durand, I. Cavero-Pelaez, H.B. Chan, D.A.R. Dalvit, R.S. Decca, G. Dufour, T. Ebbesen, E. Fischbach, C. Genet, R. Guérout, G.-L. Ingold, F. Intravaia, M.-T. Jaekel, A. Liscio, J. Lussange, P.A. Maia Neto, K.A. Milton, V.V. Nesvizhevsky, G. Palasantzas, P. Samori, C. Speake, A. Voronin and Y. Zeng for contributions or discussions related to this paper, and the ESF Research Networking Programme CASIMIR (www.casimir-network.com) for providing excellent opportunities for discussions on the Casimir effect and related topics.

[1] P.W. Milonni, *The quantum vacuum* (Academic, 1994).
[2] K.A. Milton, *The Casimir effect, physical manifestation of zero-point energy* (World Scientific, 2001).
[3] C. Itzykson and J.-B. Zuber, *Quantum Field Theory* (McGraw Hill, 1985).
[4] C. Cohen-Tannoudji, J. Dupont-Roc and G. Grynberg, *Atom-Photon Interactions* (Wiley, 1992).
[5] H.B.G. Casimir, *Proc. K. Ned. Akad. Wet. (Phys.)* **51** 79 (1948).
[6] S.K. Lamoreaux, *Resource Letter CF-1: Casimir Force* in *Am. J. Phys.* **67** 850 (1999).
[7] R.S. Decca, E. Fischbach, G.L. Klimchitskaya *et al*, *Phys. Rev. D* **68** 116003 (2003).
[8] R.S. Decca, D. López, E. Fischbach *et al*, *Annals Phys.* **318** 37 (2005).
[9] R.S. Decca, D. López, E. Fischbach *et al*, *Phys. Rev. D* **75** 077101 (2007).
[10] R.S. Decca, D. López, E. Fischbach *et al*, *Eur. Phys. J.* **C 51** 963 (2007).
[11] R.G. Barrera and S. Reynaud eds., *Focus on Casimir Forces* in *New J. Phys.* **8** (2006).
[12] G.L. Klimchitskaya, U. Mohideen and V.M. Mostepanenko, *Rev. Mod. Phys.* **81** 1827 (2009).
[13] D.A.R. Dalvit, P.W. Milonni, D.C. Roberts and F.S.S. Rosa eds., *Casimir physics*, Lecture Notes in Physics **834** (Springer-Verlag, 2011).
[14] M.T. Jaekel and S. Reynaud, *Rep. Progr. Phys.* **60** 863 (1997).
[15] R. Balian, *Séminaire Poincaré* **1** (Birkhäuser, 2003) p.55.
[16] E. Fischbach and C. Talmadge, *The Search for Non Newtonian Gravity* (AIP Press/Springer-Verlag, 1998).
[17] E.G. Adelberger, B.R. Heckel and A.E. Nelson, *Ann. Rev. Nucl. Part. Sci.* **53** 77 (2003).
[18] E.G. Adelberger, J.H. Gundlach, B.R. Heckel, S. Hoedl and S. Schlamminger, *Progr. Particle Nuclear Phys.* **62** 102 (2009).
[19] I. Antoniadis, S. Baessler, M. Büchner *et al*, *C. R. Physique* **12** 755 (2011).
[20] A. Lambrecht and S. Reynaud, *Séminaire Poincaré* **1** 107 (Birkhäuser, 2003).
[21] H.B.G. Casimir and D. Polder, *Phys. Rev.* **73** 360 (1948).
[22] G. Feinberg and J. Sucher, *Phys. Rev. A* **2** 2395 (1970).
[23] E.A. Power and T. Thirunamachandran, *Chem. Phys.* **171** 1 (1993).
[24] K.A. Milton, *Resource Letter VWCPF-1: van der Waals and Casimir-Polder forces* in *Am. J. Phys.* **79** 697 (2011).
[25] F. Intravaia, C. Henkel and M. Antezza in *Casimir physics*, D.A.R. Dalvit, P.W. Milonni, D.C. Roberts and F.S.S. Rosa eds., Lecture Notes in Physics **834** (Springer-Verlag, 2011) p.345.
[26] V.A. Parsegian, *Van der Waals Forces: a Handbook for Biologists, Chemists, Engineers, and Physicists* (Cambridge University Press, 2006).
[27] R.H. French, V.A. Parsegian, R. Podgornik *et al*, *Rev. Mod. Phys.* **82** 1887 (2010).
[28] M.-T. Jaekel and S. Reynaud, *J. Physique I* **1** 1395 (1991).
[29] A. Lambrecht and S. Reynaud, *Euro. Phys. J.* **D 8** 309 (2000).
[30] C. Genet, A. Lambrecht and S. Reynaud, *Phys. Rev. A* **67** 043811 (2003).
[31] E.M Lifshitz, *Sov. Phys. JETP* **2** 73 (1956).
[32] I.E. Dzyaloshinskii, E.M. Lifshitz and L.P. Pitaevskii, *Sov. Phys. Uspekhi* **4** 153 (1961).
[33] E.M. Lifshitz and L.P. Pitaevskii, *Landau and Lifshitz Course of Theoretical Physics: Statistical Physics Part 2* (Butterworth-Heinemann, 1980).
[34] A. Lambrecht, P.A. Maia Neto and S. Reynaud, *New J. Phys.* **8** 243 (2006).
[35] T. Emig, N. Graham, R. L. Jaffe, and M. Kardar, *Phys. Rev. Lett.* **99** 170403 (2007).
[36] K.A. Milton and J. Wagner, *J. Phys. A* **41** 155402 (2008).
[37] A. Lambrecht, A. Canaguier-Durand, R. Guérout and S. Reynaud, in *Casimir physics*, D.A.R. Dalvit, P.W. Milonni, D.C. Roberts and F.S.S. Rosa eds., Lecture Notes in Physics **834** (Springer-Verlag, 2011) p.97.
[38] S.J. Rahi, T. Emig and R.L. Jaffe, in *Casimir physics*, D.A.R. Dalvit, P.W. Milonni, D.C. Roberts and F.S.S. Rosa eds., Lecture Notes in Physics **834** (Springer-Verlag, 2011) p.129.
[39] A.W. Rodriguez, F. Capasso and S.G. Johnson, *Nature Photonics* **5** 211 (2011).
[40] M. Planck, *Verh. Deutsch. Phys. Ges.* **2** 237 (1900).
[41] O. Darrigol, *Ann. Physik* **9** 951 (2000).

[42] M. Planck, *Verh. Deutsch. Phys. Ges.* **13** 138 (1911).
[43] P.W. Milonni and M.-L. Shih, *Am J. Phys.* **59** 684 (1991).
[44] A. Einstein and O. Stern, *Ann. Physik* **40** 551 (1913).
[45] P. Debye, *Ann. Physik* **43** 49 (1914).
[46] R.S. Mulliken, *Nature* **114** 349 (1924).
[47] S. Reynaud, *Ann. Physique* **15** 63 (1990).
[48] S. Reynaud, A. Heidmann, E. Giacobino and C. Fabre, *Progress in Optics* **30** 1 (1992).
[49] C. Fabre *et al* eds, *Quantum Optics and Nanophotonics*, Les Houches Summer School, August 2913 to appear (Oxford Univ. Press, 2014).
[50] W. Nernst, *Verh. Deutsch. Phys. Ges.* **18** 83 (1916).
[51] P.F. Browne, *Apeiron* **2** 72 (1995).
[52] S. Weinberg, *Rev. Mod. Phys.* **61** 1 (1989).
[53] R.J. Adler, B. Casey, and O. C. Jacob, *Am. J. Phys.* **63** 620 (1995)
[54] W. Pauli, *Handbuch der Physik* **24** 1 (1933).
[55] C.P. Enz, in *Physical Reality and Mathematical Description*, C.P. Enz and J. Mehra eds (Reidel, 1974) p.124.
[56] J. Schwinger, *Lett. Math. Phys.* **1** 43 (1975).
[57] I.J.R. Aitchinson, *Contemporary Physics* **26** 331 (1985).
[58] S. Saunders, and H.R. Brown, in *The philosophy of vacuum*, S. Saunders ed. (Clarendon Press, 1991) p.27.
[59] D.W. Sciama, in *The philosophy of vacuum*, S. Saunders ed. (Clarendon Press, 1991) p.137.
[60] S.E. Rugh and H. Zinkernagel, *Stud. Hist. Phil. Mod. Phys.* **33** 663 (2002).
[61] R.L. Jaffe, *Phys. Rev. D* **72** 021301(R) (2005) .
[62] H. Kragh, *Archive for History of Exact Sciences* **66** 199 (2012).
[63] H. Kragh, *Astronomy & Geophysics* **53** 1.24 (2012).
[64] A.G. Riess, A.V. Filippenko, P Challis *et al*, *Astron. J.* **116** 1009 (1998).
[65] S. Perlmutter, G. Aldering, G. Goldhaber *et al*, *Astrophys. J.* **517** 565 (1999).
[66] C.L. Bennett, M. Halpern, G. Hinshaw *et al*, *Astrophys. J. Suppl. Ser.* **148** 1 (2003).
[67] S.R. Beane, *Gen. Relativ. Gravit.* **29** 945 (1997).
[68] G. Dvali, G. Gabadadze, M. Kolanovic and F. Nitti, *Phys. Rev. D* **65** 024031 (2001).
[69] R. Sundrum, *Phys. Rev. D* **69** 044014 (2004).
[70] D.J. Kapner, T.S. Cook, E.G. Adelberger *et al*, *Phys. Rev. Lett.* **98** 021101 (2007).
[71] N. Arkani-Hamed, S. Dimopoulis and G. R. Dvali, *Phys. Lett. B* **436** 257 (1998).
[72] A. Lambrecht and S. Reynaud, *Int. J. Mod. Phys. A* **27** 1260013 (2012).
[73] V.B. Svetovoy, P.J. van Zwol, G. Palasantzas and J.Th.M. De Hosson, *Phys. Rev. B* **77** 035439 (2008).
[74] E.D. Palik ed., *Handbook of Optical Constants of Solids* (Academic Press, 1995).
[75] N.W. Ashcroft and N.D. Mermin, *Solid State Physics* (HRW International, 1976).
[76] J. Mehra, *Physica* **37** 145 (1967).
[77] L.S. Brown and G.J. Maclay, *Phys. Rev.* **184** 1272 (1969).
[78] J. Schwinger, L.L. de Raad and K.A. Milton, *Ann. Phys.* **115** 1 (1978).
[79] C. Genet, A. Lambrecht and S. Reynaud, *Phys. Rev. A* **62** 012110 (2000).
[80] K.A. Milton, *J. Phys. A* **20** 4628 (2005).
[81] G.L. Klimchitskaya and V.M. Mostepanenko, *Contemp. Phys.* **47** 131 (2006).
[82] I. Brevik, S.A. Ellingsen and K. Milton, *New J. Phys.* **8** 236 (2006).
[83] G.-L. Ingold, A. Lambrecht and S. Reynaud, *Phys. Rev. E* **80** 041113 (2009).
[84] I. Brevik and J.S. Hoye, *Eur. J. Phys.* **35** 015012 (2014).
[85] M. Boström and B.E. Sernelius, *Phys. Rev. Lett.* **84** 4757 (2000).
[86] B. Jancovici and L. Šamaj, *Europhys. Lett.* **72** 35 (2005).
[87] P.R. Buenzli and P.A. Martin, *Europhys. Lett.* **72** 42 (2005).
[88] G. Bimonte, *Phys. Rev. A* **79** 042107 (2009).
[89] B.V. Deriagin, I.I. Abrikosova and E.M. Lifshitz, *Quart. Rev.* **10** 295 (1968).
[90] R.S. Decca, E. Fischbach, G.L. Klimchitskaya *et al*, *Phys. Rev. D* **79** 124021 (2009).
[91] C.-C. Chang, A.A. Banishev, R. Castillo-Garza *et al*, *Phys. Rev. B* **85** 165443 (2012).
[92] A.O. Sushkov, W.J. Kim, D.A.R. Dalvit and S.K. Lamoreaux, *Nature Physics* **7** 230 (2011).
[93] B.V. Derjaguin, I.I. Abrikosova and E. M. Lifshitz, *Q. Rev. Chem. Soc.* **10** 295 (1956).
[94] M. J. Sparnaay, *Physica* **24** 751 (1958).
[95] E.S. Sabisky and C.H. Anderson, *Phys. Rev. A* **7** 790 (1973).
[96] S.K. Lamoreaux, *Phys. Rev. Lett.* **78** 5 (1997).
[97] U. Mohideen and A. Roy, *Phys. Rev. Lett.* **81** 4549 (1998).
[98] B.W. Harris, F. Chen and U. Mohideen, *Phys. Rev. A* **62** 052109 (2000).
[99] T. Ederth, *Phys. Rev.* **A 62** 062104 (2000).
[100] H.B. Chan, V.A. Aksyuk, R.N. Kleiman, D.J. Bishop and F. Capasso, *Phys. Rev. Lett.* **87** 211801 (2001).
[101] G. Bressi, G. Carugno, R. Onofrio and G. Ruoso, *Phys. Rev. Lett.* **88** 041804 (2002).
[102] M. Lisanti, D. Iannuzzi and F. Capasso, *Proc. Nat. Ac. Sci. USA* **102** 11989 (2005).
[103] R.S. Decca, D. López, H.B. Chan *et al*, *Phys. Rev. Lett.* **94** 240401 (2005).
[104] W.J. Kim, M. Brown-Hayes, D.A.R Dalvit, J.H. Brownell and R. Onofrio, *Phys. Rev.* **A 78** 020101(R) (2008).
[105] G. Jourdan, A. Lambrecht, F. Comin and J. Chevrier, *Euro. Phys. Lett.* **85** 31001 (2009).
[106] S. de Man, K. Heeck and D. Iannuzzi, *Phys. Rev.* **A 79** 024102 (2009).
[107] M. Masuda and M. Sasaki, *Phys. Rev. Lett.* **102** 171101 (2009).
[108] J. N. Munday, F. Capasso, and V. A. Parsegian, *Nature* **457** 170 (2009).
[109] G. Torricelli, P.J. van Zwol, O. Shpak *et al*, *Phys. Rev. A* **82** 010101 (2010).
[110] A.A. Banishev, C.-C. Chang, G. L. Klimchitskaya, V.M. Mostepanenko and U. Mohideen, *Phys. Rev. B* **85** 195422 (2012).
[111] A.A. Banishev, G.L. Klimchitskaya, V.M. Mostepanenko and U. Mohideen, *Phys. Rev. Lett.* **110** 137401 (2013).
[112] R. Castillo-Garza, J. Xu, G.L. Klimchitskaya, V.M. Mostepanenko and U. Mohideen, *Phys. Rev. B* **85** 075402 (2013).
[113] R.S. Decca, slides of the talk at the PASI school *Frontiers of Casimir Physics* (Ushuaia, 2012) http://physics.iupui.edu/graduate/program

[114] K. Milton, *Nature Physics* **7** 190 (2011).
[115] R.O. Behunin, F. Intravaia, D.A.R. Dalvit, P.A. Maia Neto and S. Reynaud, *Phys. Rev. A* **85** (2012) 012504.
[116] L.P. Pitaevskii, *Phys. Rev. Lett.* **101** 163202 (2008).
[117] D.A.R. Dalvit and S.K. Lamoreaux, *Phys. Rev. Lett.* **101** 163203 (2008).
[118] V.B. Svetovoy, *Phys. Rev. Lett.* **101** 163603 (2008); *Phys. Rev. Lett.* **102** 219903(E) (2009).
[119] B. Geyer, G.L. Klimchitskaya, U. Mohideen and V.M. Mostepanenko, *Phys. Rev. Lett.* **102** 189301 (2009).
[120] L.P. Pitaevskii, *Phys. Rev. Lett.* **102** 189302 (2009).
[121] R.S. Decca, E. Fischbach, B. Geyer *et al*, *Phys. Rev. Lett.* **102** 189303 (2009).
[122] D.A.R. Dalvit and S.K. Lamoreaux, *Phys. Rev. Lett.* **102** 189304 (2009).
[123] A. Canaguier-Durand, R. Guérout, P.A. Maia Neto, A. Lambrecht and S. Reynaud, *Int. J. Mod. Phys. Conf. Series* **14** 250 (2012).
[124] P.A. Maia Neto, A. Lambrecht and S. Reynaud, *Europhys. Lett.* **69** 924 (2005); *EPL* **100** 29902(E) (2012).
[125] P.A. Maia Neto, A. Lambrecht and S. Reynaud, *Phys. Rev. A* **72** 012115 (2005); *Phys. Rev. A* **A 86** 059901(E) (2012).
[126] P.J. van Zwol, V.B. Svetovoy and G. Palasantzas, *Phys. Rev. B* **80** 235401 (2009).
[127] W. Broer, G. Palasantzas, J. Knoester and V.B. Svetovoy, *EPL* **95** 30001 (2011).
[128] W. Broer, G. Palasantzas, J. Knoester and V.B. Svetovoy, *Phys. Rev. B* **85** 155410 (2012).
[129] W. Broer, G. Palasantzas, J. Knoester and V.B. Svetovoy, *Phys. Rev. B* **87** 125413 (2013).
[130] F. C. Witteborn and W. M. Fairbank, *Phys. Rev. Lett.* **19** 1049 (1967).
[131] J.B. Camp, T.W. Darling and R.E. Brown, *J. Appl. Phys.* **69** 7126 (1991).
[132] V. Sandoghdar, C.I. Sukenik, S. Haroche and E.A. Hinds, *Phys. Rev. A* **53** 1919 (1996).
[133] Q.A. Turchette, D. Kielpinski, B.E. King *et al*, *Phys. Rev. A* **61** 063418 (2000).
[134] L. Deslauriers, S. Olmschenk, D. Stick *et al*, *Phys. Rev. Lett.* **97** 103007 (2006).
[135] N.A. Robertson, J.R. Blackwood, S. Buchman *et al*, *Class. Quantum Grav.* **23** 2665 (2006).
[136] R.J. Epstein, S. Seidelin, D. Leibfried *et al*, *Phys. Rev. A* **76** 033411 (2007).
[137] S.E. Pollack, S. Schlamminger and J.H. Gundlach, *Phys. Rev. Lett.* **101** 071101 (2008).
[138] R. Dubessy, T. Coudreau and L. Guidoni, *Phys. Rev. A* **80** 031402 (2009).
[139] J.D. Carter and J.D.D. Martin, *Phys. Rev. A* **83** 032902 (2011).
[140] C.W.F. Everitt, D.B. DeBra, B.W. Parkinson *et al*, *Phys. Rev. Lett.* **106** 221101 (2011).
[141] R.D. Reasenberg, E.C. Lorenzini, B.R. Patla *et al*, *Class. Quantum Grav.* **28** 094014 (2011).
[142] D.A. Hite, Y. Colombe, A.C. Wilson *et al*, *Phys. Rev. Lett.* **109** 103001 (2012).
[143] D.A. Hite, Y. Colombe, A.C. Wilson *et al*, *MRS Bulletin* **38** 826 (2013).
[144] C.C. Speake and C. Trenkel, *Phys. Rev. Lett.* **90** 160403 (2003).
[145] A.A. Chumak, P.W. Milonni and G.P. Berman, *Phys. Rev. B* **70** 085407 (2004).
[146] W.J. Kim, A.O. Sushkov, D.A.R. Dalvit and S.K. Lamoreaux, *Phys. Rev. A* **81** 022505 (2010).
[147] W.J. Kim and U.D. Schwarz, *J. Vac. Sci. Technol. B* **28** C4A1 (2010).
[148] S. de Man, K. Heeck, R.J. Wijngaarden and D. Iannuzzi, *J. Vac. Sci. Technol. B* **28** C4A25 (2010).
[149] N. Gaillard, M. Gros-Jean, D. Mariolle, F. Bertin and A. Bsiesy, *Appl. Phys. Lett.* **89** 154101 (2006).
[150] F. Rossi and G. I. Opat, *J. Appl. Phys. D* **25** 1349 (1992).
[151] A. Liscio, V. Palermo, K. Müllen and P. Samori, *J. Phys. Chem. C* **112** 17368 (2008).
[152] A. Liscio, V. Palermo and P. Samori, *Accounts Chem. Res.* **43** 541 (2010).
[153] R.O. Behunin, D.A.R. Dalvit, R.S. Decca *et al*, arXiv:1407.3741.
[154] R.O. Behunin, Y. Zeng, D.A.R. Dalvit, and S. Reynaud, *Phys. Rev. A* **86** 052509 (2012).
[155] B.A. Lippmann and J. Schwinger, *Phys. Rev.* **79** 469 (1950).
[156] M. Gell-Mann and M.L. Goldberger, *Phys. Rev.* **91** 398 (1953).
[157] G. Plunien, B. Müller and W. Greiner, *Phys. Rep.* **134** 87 (1986).
[158] P.W. Milonni, R.J. Cook and M.E. Goggin, *Phys. Rev. A* **38** 1621 (1988).
[159] M.-T. Jaekel and S. Reynaud, *Quantum Optics* **4** 39 (1992).
[160] M.-T. Jaekel and S. Reynaud, *J. Physique I* **2** 149 (1992).
[161] M.-T. Jaekel and S. Reynaud, *Phys. Lett. A* **167** 227 (1992).
[162] M.-T. Jaekel and S. Reynaud, *J. Physique I* **3** 1 (1993).
[163] M.-T. Jaekel and S. Reynaud, *J. Physique I* **3** 1093 (1993).
[164] M.-T. Jaekel and S. Reynaud, *Phys. Lett. A* **172** 319 (1993).
[165] A. Lambrecht, M.-T. Jaekel and S. Reynaud, *Phys. Rev. Lett.* **77** 615 (1996).
[166] A. Lambrecht, M.-T. Jaekel and S. Reynaud, *Eur. Phys. J D* **3** 95 (1998).
[167] R. Guérout, A. Lambrecht, K. Milton, and S. Reynaud, to appear in *Phys. Rev. E* (2014) [arXiv:1404.7633].
[168] T. Matsubara, *Prog. Theor. Phys.* **14** 351 (1955).
[169] C. Cohen-Tannoudji, J. Dupont-Roc and G. Grynberg, *Photons and Atoms* (Wiley, 1989).
[170] S.M. Barnett, C.R. Gilson, B. Huttner and N. Imoto, *Phys. Rev. Lett.* **77** 1739 (1996).
[171] S.M. Barnett, J. Jeffers, A. Gatti and R. Loudon, *Phys. Rev. A* **57** 2134 (1998).
[172] J.M. Courty, F. Grassia and S. Reynaud, in *Noise, Oscillators and Algebraic Randomness*, ed. M. Planat (Springer, 2000) p.71.
[173] M. Born and E. Wolf, *Principles of Optics* (Cambridge University Press, 1999).
[174] L. Landau, E.M. Lifshitz and L.P. Pitaevskii, *Landau and Lifshitz Course of Theoretical Physics: Electrodynamics in Continuous Media* (Butterworth-Heinemann, 1980).
[175] E.I. Kats, *JETP* **46** 109 (1977).
[176] D. Langbein *Phys. Rev. B* **2** 3371 (1970).
[177] M.J. Renne, *Physica* **56** 125 (1971).
[178] P. Candelas, *Ann. Phys.* **143** 241 (1982).
[179] D. Kupiszewska and J. Mostowski, *Phys. Rev. A* **41** 4636 (1990).

[180] S. Scheel and S.Y. Buhmann, *Acta Physica Slovaca* **58** 675 (2008).

[181] O. Kenneth and I. Klich, *Phys. Rev. B* **78** 014103 (2008).

[182] S.J. Rahi, T. Emig, N. Graham, R.L. Jaffe and M. Kardar, *Phys. Rev. D* **80** 085021 (2009).

[183] F. Intravaia and R. Behunin, *Phys. Rev. A* **86** 062517 (2012).

[184] M.T.H. Reid, J. White and S.G. Johnson, *Phys. Rev. A* **88** 022514 (2013).

[185] R. Balian and B. Duplantier, *Ann. Phys.* **104** 300 (1977).

[186] R. Balian and B. Duplantier, *Ann. Phys.* **112** 165 (1978)

[187] M. Schaden and L. Spruch, *Phys. Rev. Lett.* **84** 459 (2000).

[188] R.L. Jaffe and A. Scardicchio, *Phys. Rev. Lett.* **92** 070402 (2004).

[189] O. Schröder, A. Sardicchio and R.L. Jaffe, *Phys. Rev. A* **72** 012105 (2005).

[190] F. Chen, U. Mohideen, G.L. Klimchitskaya and V.M. Mostepanenko, *Phys. Rev. Lett.* **88** 101801 (2002).

[191] R. Büscher and T. Emig, *Phys. Rev. Lett.* **94** 133901 (2005).

[192] R.B. Rodrigues, P.A. Maia Neto, A. Lambrecht and S. Reynaud, *Phys. Rev. Lett.* **96** 100402 (2006); see also *Phys. Rev. Lett.* **98** 068902 (2007).

[193] R.B. Rodrigues, P.A. Maia Neto, A. Lambrecht and S. Reynaud, *Phys. Rev. A* **75** 062108 (2007).

[194] H.B. Chan, Y. Bao, J. Zou *et al*, *Phys. Rev. Lett.* **101** 030401 (2008).

[195] H.C. Chiu, G.L. Klimchitskaya, V.N. Marachevsky *et al*, *Phys. Rev. A* **80** 121402 (2009).

[196] F. Intravaia, S. Koev, I. Woong Jung *et al*, *Nature Comm.* **4** 2515 (2013).

[197] A. Lambrecht and V.N. Marachevsky, *Phys. Rev. Lett.* **101** 160403 (2008).

[198] A. Lambrecht, *Nature* **454** 836 (2008).

[199] Y. Bao, R. Guérout, J. Lussange *et al*, *Phys. Rev. Lett.* **105** 250402 (2010).

[200] R. Guérout, J. Lussange, H.B. Chan, A. Lambrecht and S. Reynaud, *Phys. Rev. A* **87** 052514 (2013).

[201] R.B. Rodrigues, P.A. Maia Neto, A. Lambrecht and S. Reynaud, *Europhys. Lett.* **76** 822 (2006).

[202] S. Reynaud, P.A. Maia Neto and A. Lambrecht, *J. Phys. A* **41** 164004 (2008).

[203] T. Emig and R.L. Jaffe, *J. Phys. A* **41** 164001 (2008)

[204] M. Bordag, and V. Nikolaev, *J. Phys. A* **41** 164002 (2008)

[205] A. Wirzba, *J. Phys. A* **41** 164003 (2008)

[206] K. Klingmüller and H. Gies, *J. Phys. A* **41** 164042 (2008)

[207] P.A. Maia Neto, A. Lambrecht and S. Reynaud, *Phys. Rev. A* **78** 012115 (2008).

[208] T. Emig, *J. Stat. Mech.: Theory Exp.* P04007 (2008).

[209] A. Canaguier-Durand, P.A. Maia Neto, I. Cavero-Pelaez *et al*, *Phys. Rev. Lett.* **102** 230404 (2009).

[210] A. Canaguier-Durand, P.A. Maia Neto, A. Lambrecht and S. Reynaud, *Phys. Rev. Lett.* **104** 040403 (2010).

[211] A. Canaguier-Durand, P.A. Maia Neto, A. Lambrecht and S. Reynaud, *Phys. Rev. A* **82** 012511 (2010); *Phys. Rev. A* **83** 039905(E) (2011).

[212] D.E. Krause, R.S. Decca, D. López and E. Fischbach, *Phys. Rev. Lett.* **98** 050403 (2007).

[213] C.D. Fosco, F.C. Lombardo and F.D. Mazzitelli, *Phys. Rev. D* **84** 105031 (2011).

[214] G. Bimonte, T. Emig and M. Kardar, *Appl. Phys. Lett.* **100** 074110 (2012).

[215] G. Bimonte, T. Emig, R.L. Jaffe and M. Kardar, *EPL* **97** 50001 (2012).

[216] A. Canaguier-Durand, G.-L. Ingold, M.-T. Jaekel *et al*, *Phys. Rev. A* **85** 052501 (2012).

[217] G. Bimonte and T. Emig, *Phys. Rev. Lett.* **109** 160403 2012.

[218] A. Canaguier-Durand, A. Gérardin, R. Guérout *et al*, *Phys. Rev. A* **83** 032508 (2011).

[219] R. Messina, D.A.R. Dalvit, P.A. Maia Neto, A. Lambrecht and S. Reynaud, *Phys. Rev. A* **80** 022119 (2009).

[220] D.A.R. Dalvit, P.A. Maia Neto, A. Lambrecht and S. Reynaud, *Phys. Rev. Lett.* **100** 040405 (2008).

[221] A.M. Contreras-Reyes, R. Guérout, P.A. Maia Neto *et al*, *Phys. Rev. A* **82** 052517 (2010).

[222] F. Impens, A.M. Contreras-Reyes, P.A. Maia Neto *et al*, *EPL* **92** 40010 (2010).